Supporting Information

A Dioxygen-Derived Nonheme Mononuclear $Fe^{III}(OH)$ Complex and its Reactivity with Carbon Radicals

Vishal Yadav, Jesse B. Gordon, Maxime A. Siegler, David P. Goldberg*

Department of Chemistry, The Johns Hopkins University, Baltimore, Maryland 21218, United States

Contents

A. Materials and Instrumentation:

Materials. All syntheses and manipulations were conducted in an N_2-filled drybox (Vacuum Atmospheres, O_2 < 0.2 ppm, H_2O < 0.5 ppm) or using standard Schlenk techniques under an atmosphere of Ar unless otherwise noted. $Fe(OTf)_2$•2MeCN and $^{57}Fe(OTf)_2$•2MeCN were prepared according to a literature procedure.[1] Powdered ^{57}Fe metal (95.93%) was purchased from Cambridge Isotope Laboratories. The isotopically labelled $^{18}O_2$ (98 atom %) was purchased from ICON Isotopes (Summit, N.J.) and $H_2{}^{18}O$ (99 atom %) was purchased from Sigma-Aldrich in a serum bottle. Acetonitrile and acetonitrile-d_3 were distilled from CaH_2. Tetrahydrofuran, tetrahydrofuran-d_8, toluene and toluene-d_8 were dried over Na/benzophenone and subsequently distilled. All other non-deuterated solvents were obtained from a Pure-solv solvent purification system from Innovative Technologies, Inc. Anhydrous pentane (sure seal) was purchased from Sigma-Aldrich and was distilled over Na/benzophenone. Anhydrous carbon tetrachloride (CCl_4) (sure seal) was purchased from Sigma-Aldrich and used without further purification. All solvents were degassed by a minimum of three freeze−pump−thaw cycles and stored over freshly activated 3 Å molecular sieves in the drybox following distillation. All other reagents were purchased from commercial vendors and used without further purification except N-bromosuccinimide, which was recrystallized from hot water. The compounds 2-amino-1,1-diphenylethanol,[2] tris(*p*-methoxyphenyl)methyl radical,[3] and Gomberg's dimer[4] ($(Ph_3C)_2$) were synthesized following literature procedures.

Instrumentation. The ^1H, ^{13}C, and ^{19}F NMR spectra were measured on a Bruker 300 MHz or a Bruker 400 MHz spectrometer. Chemical shifts were referenced to reported solvent resonances.[5] UV−vis experiments were carried out on an Agilent 5453 diode-array spectrophotometer using a 1 cm cuvette. Midwest Microlab LLC (Indianapolis, IN) conducted elemental analyses on samples prepared and shipped in ampules sealed under vacuum. ESI mass spectra were acquired using a Finnigan LCQ Duo ion-trap mass spectrometer

equipped with an electrospray ionization source (Thermo Finnigan, San Jose, CA). Mössbauer spectra were recorded on a spectrometer from SEE Co. (Edina, MN) operating in the constant acceleration mode in a transmission geometry. The sample was kept in an SVT-400 cryostat from Janis Research Co. (Wilmington, MA), using liquid He as a cryogen for 5 K data collection and liquid N_2 as a cryogen for 80 K measurements. Isomer shifts were determined relative to the centroid of the spectrum of a metallic foil of α-Fe collected at room temperature. Data analysis was performed using version F of the program WMOSS (www.wmoss.org), and quadrupole doublets were fit to Lorentzian lineshapes. Electron paramagnetic resonance (EPR) spectra were recorded with a Bruker EMX spectrometer equipped with a Bruker ER 041 X G microwave bridge and a continuous-flow liquid helium cryostat (ESR900) coupled to an Oxford Instruments TC503 temperature controller for low temperature data collection. Cyclic voltammetry was performed on an EG&G Princeton Applied Research potentiostat/galvanostat model 263A with a three-electrode system consisting of a glassy carbon working electrode, a $Ag/AgNO_3$ non-aqueous reference electrode (0.01 M $AgNO_3$ with 0.1 M Bu_4NOTf in CH_3CN), and a platinum wire counter electrode. Potentials were referenced using an external ferrocene standard. Scans were run inside a N_2-filled drybox at 23 ˚C using Bu_4NOTf (0.1 M) as the supporting electrolyte.

B. Synthesis.

Synthesis of BNPA^{Ph_2}OH.

6-pivaloylamino-2-picoline. The synthesis was performed according to a literature procedure with a few modifications.[6] The starting material 2-amino-6-methylpyridine (28.0 g, 0.27 mol) was dissolved in dry CH_2Cl_2 (300 mL) and triethylamine (39 mL, 0.28 mol) was added slowly at 0 °C and stirred for 30 min. Trimethylacetylchloride (34 mL, 0.28 mol) was added slowly over the course of 30 min at 0 °C with constant stirring (*caution : HCl vapor is a byproduct and needs to be safely released through proper venting of the reaction vessel*), and the reaction mixture was additionally stirred for 2 h at 0 °C. The reaction mixture was warmed to 23 °C and stirred again for an additional 2 h. The reaction mixture was then filtered to remove a white precipitate, resulting in a dark yellow filtrate. The white precipitate was washed with hexanes and the organics were combined. Solvent was removed under *vacuo* to obtain a light yellow solid. The solid was dissolved in CH_2Cl_2 and passed through a neutral alumina column using CH_2Cl_2 as eluent. The solvent was removed to afford a pale yellow solid, which was then dissolved in THF and stirred for 15 min. The turbid solution was then filtered through Celite to remove any remaining triethylammonium chloride. Then the clear yellow filtrate was dried under reduced pressure to give a pure, microcrystalline, off-white solid; 47.7 g (92%). ^{1}H NMR ($CDCl_3$, 400 MHz): δ 8.05-8.03 (d, 1H), 7.94 (s, 1H, br), 7.55-7.59 (t, 1H), 6.86-6.88 (d, 1H), 2.44 (s, 3H), 1.32 (s, 9H) ppm.

(6-bromomethyl-pyridin-2-yl)pivalamide. The synthesis was performed according to a literature procedure.[6] An amount of 6-pivaloylamino-2-picoline (2.20 g, 10.4 mmol) was dissolved in dry CCl_4 (40 mL). To the resulting pale yellow solution N-bromosuccinimide (3.70 g, 20.8 mmol) and AIBN (200 mg, 4.16 mmol) were added and the reaction was set to reflux for 8 h. The reaction mixture was cooled to 23 °C, and a brown precipitate formed, along with a dark orange solution. The solution was filtered over Celite, and then the Celite washed with CH_2Cl_2. The combined dark orange organic filtrate was washed three times with saturated $NaHCO_3$ solution and then washed

twice with brine. The clear, dark golden-yellow organic layers were combined and dried over $MgSO_4$, filtered, and then the volatiles were removed under *vacuo* to give a dark brown oil. The brown oil was dried under vacuum for 12 h. The product was purified by silica gel column chromatography using EtOAc/hexanes (15/85 v/v) as eluent to give a pure yellow solid; 1.26 g (45%). ^{1}H NMR ($CDCl_3$, 400 MHz): δ 8.17 (d, 1H); 8.00 (s, 1H, br); 7.69 (t, 1H); 7.13 (d, 1H), 4.43 (s, 2H), 1.34 (s, 9H) ppm.

BPPA^{Ph_2}OH. The starting material (6-bromomethyl-pyridin-2-yl)pivalamide (1.00 g, 3.70 mmol) was dissolved in dry acetonitrile (100 mL), K_2CO_3 (464 mg, 3.36 mmol) was added, and the solution was stirred for 15 min. An amount of 2-amino-1,1-diphenylethanol (375 mg, 1.76 mmol) was added in one portion and the yellow reaction mixture was refluxed for 24 h. The reaction mixture was cooled to 23 ºC which formed a dark orange solution along with a white solid. The white solid was filtered through Celite, and the Celite was washed with acetonitrile. The filtrate was dried under *vacuo*, giving an oil. The product was purified by neutral alumina column using EtOAc/hexanes (50/50 v/v) as eluent to give a white solid; 770 mg (70%). ^{1}H NMR ($CDCl_3$, 400 MHz): δ 8.07 (d, 4H), 7.56-7.48 (m, 7H), 7.30-7.25 (m, 3H), 7.19-7.15 (m, 2H), 6.72 (d, 2H), 3.74 (s, 2H), 3.70 (s, 4H), 1.37 (s, 18H) ppm. ^{13}C NMR ($CDCl_3$, 100 MHz): δ 177.04, 157.66, 150.72, 147.64, 138.71, 128.00, 126.56, 126.11, 118.32, 111.93, 66.29, 60.85, 39.83, 27.52 ppm.

BNPA^{Ph_2}OH. Lithium aluminum hydride (37.0 mg, 4.64 mmol) was added to anhydrous diethyl ether (60 mL) at 0 ºC and stirred for 10 min. Then solid BPPA^{Ph_2}OH (459 mg, 0.77 mmol) was added to this suspension causing vigorous bubbling, and the suspension was stirred for an additional 30 min. The reaction warmed to 23 ºC and stirred again for 18 h. The reaction mixture turned to dark orange over this time and was quenched with a few drops of distilled water. The reaction mixture was extracted with ethyl acetate, washed with brine, and dried over Na_2SO_4. The volatiles were removed under *vacuo* to obtain a dark yellow oil, which was purified by neutral alumina

column using EtOAc/hexanes (30/70 v/v) as eluent to give a pale yellow oil; 392 mg (90%). ^{1}H NMR ($CDCl_3$, 400 MHz): δ 7.56 (d, 4H), 7.28-7.24 (m, 6H), 7.17 (t, 2H); 6.36 (d, 2H), 6.26 (d, 2H), 3.76 (s, 2H), 3.62 (s,4H), 3.12 (d,4H), 1.03 (s,18H) ppm. ^{13}C NMR ($CDCl_3$, 100 MHz): δ 158.93, 157.88, 147.54, 137.62, 127.79, 126.40, 111.58, 104.22, 67.99, 65.58, 60.58, 53.90, 32.15, 27.56 ppm. λ_{max} (CH_3CN) = 311 nm.

Synthesis of metal complexes.

$Fe^{II}(BNPA^{Ph_2}O)(OTf)$ (1). The ligand $BNPA^{Ph_2}OH$ was dried over P_2O_5 for 12 h under vacuum before metalation. The ligand $BNPA^{Ph_2}OH$ (57.3 mg, 0.10 mmol) was dissolved in THF (2 mL) and a suspension of NaH (2.4 mg, 0.10 mmol) in THF was added. The solution was stirred for 1 h at 23 °C. An amount of $Fe(OTf)_2 \bullet 2\ CH_3CN$ (44.0 mg, 0.10 mmol) was dissolved in acetonitrile (2 mL) and added dropwise to the $BNPA^{Ph_2}OH$/NaH mixture. An immediate color change from colorless to yellow-green was noted, and the reaction mixture was stirred for 12 h. The resulting dark yellow reaction mixture was evaporated to dryness under vacuum giving a yellow solid. The yellow solid was dissolved in THF/CH_3CN (10/1 v/v) and filtered through Celite and the solution was left to stand with slow vapor diffusion of pentane. Yellow-green crystals (blocks, 43 mg (56%)) suitable for X-ray diffraction were obtained after 3 d. UV-vis (CH_3CN) λ_{max} (ε, M^{-1} cm^{-1}) = 323 nm (9550), 420 nm (990). *Anal. Calcd* for $C_{37}H_{46}F_3FeN_5O_4S$: C, 57.74; H, 6.02; N, 9.10. Found: C, 57.71; H, 6.02; N, 9.18. ^{1}H NMR (CD_3CN, 400 MHz): δ 97.38, 90.86, 65.72, 62.19, 35.15, 18.42, 12.09, 10.71, 8.41, 3.84, 2.10, 1.82, 0.71, -18.98 ppm.

$Fe^{III}(BNPA^{Ph_2}O)(OH)(OTf)$ (2). Crystalline **1** (30.0 mg, 0.04 mmol) was dissolved in CH_3CN (5 – 10 mL), and this solution was bubbled with excess, dry O_2 for 15 min, causing a color change from yellow to dark orange. The reaction was stirred for 4 h at 23 °C, and the final dark red solution was evaporated to dryness under vacuum to give a dark red solid. This solid was dissolved in THF

and filtered through a Celite bed to remove insoluble material. The resulting dark red filtrate was evaporated to dryness under vacuum and washed with Et_2O to give a dark red powder, which was dissolved in toluene and a minimum amount of THF, and layered with pentane. Dark orange crystals (blocks, 30.7 mg (80%)), suitable for X-ray diffraction were obtained after 2 d. UV-vis (CH_3CN) λ_{max} (ε, M^{-1} cm^{-1}) = 315 nm (9000), 365 nm (2400), 440 nm (950). ESI-MS(+): *m/z* 636.85 ([**2**-OTf]$^+$). *Anal. Calcd* for $C_{37}H_{47}F_3FeN_5O_5S$ • 0.5 C_7H_8: C, 57.50; H, 5.83; N, 8.71. Found: C, 57.53; H, 5.98; N, 8.71. ^{1}H NMR (CD_3CN, 400 MHz): δ 77.45, 21.84, 16.42, 7.21, 3.45, 2.36, 1.15 ppm. The ^{18}O-labeled complex **2(**^{18}**O)** was synthesized in the same manner, but with natural abundance O_2 replaced by $^{18}O_2$ (99%). ESI-MS(+): *m/z* 638.85 ([**2(**^{18}**O)**-OTf]$^+$).

C. Experimental Details.

Reaction of 1 and O_2 in the presence of $H_2{}^{18}O$. Crystalline **1** (2 mg) was dissolved in dry CH_3CN and $H_2{}^{18}O$ (50 μL) was added. Excess dry O_2 was added to the reaction mixture by bubbling for 15 min, which led to a color change from yellow to dark orange. The reaction mixture was analyzed by ESI-MS and showed only a major peak for unlabeled **2**, with no significant peak corresponding to ^{18}O-labeled **2.** ESI-MS(+): *m/z* 636.85 ([**2**-OTf]$^+$).

Reaction of 1 and O_2 in the presence of excess 9,10-dihydroanthracene (9,10-DHA). Crystalline **1** (15 mg, 0.019 mmol) was dissolved in CH_3CN and an amount of 9,10-DHA (34 mg, 0.19 mmol, 10 equiv) was added. The reaction mixture was sparged with dry O_2 for 10 min, and a color change from yellow to orange was noted. The reaction was analyzed by TLC (silica gel, EtOAc/hexanes (10/90 v/v)) and formation of anthracene was seen after 2 h. The CH_3CN was removed under vacuum and the resulting solids were dissolved in a minimum amount of CH_2Cl_2 and filtered through a silica gel plug to separate the organic products. The final product anthracene was further purified by silica gel chromatography (EtOAc/hexanes (5/95 v/v)) to give a white solid; 3.1 mg (90%). ^{1}H NMR ($CDCl_3$, 400 MHz): δ 8.40 (s, 2H), 7.99 (d, 4H), 7.39 (d, 4H) ppm.

The same experiment was done with **1** or **2** and excess 9,10-DHA in the absence of O_2 and no trace of anthracene was found, as seen by TLC or ^{1}H NMR. A separate control reaction involved

dissolving 9,10-DHA (20 mg, 0.11 mmol) in CH_3CN and sparging with O_2 for 15 min. This reaction also did not form any anthracene product as seen by TLC and ^{1}H NMR.

Reaction between 2 and Ph_3C•. Crystalline **2** (5.0 mg, 0.006 mmol) was dissolved in THF (5 mL) and excess $(Ph_3C)_2$ (30 mg, 0.064 mmol, 10 equiv) was added and the reaction mixture was stirred in the dark for 4 h at 23 °C. The reaction mixture turned from bright orange to dark yellow, and then was dried under vacuum to give a dark yellow solid. The residue was dissolved in CD_3CN and analyzed by ^{1}H NMR spectroscopy. The ^{1}H NMR spectrum showed complete disappearance of the broad, paramagnetically shifted peaks for the Fe^{III} complex **2**, and appearance of the relatively sharp, paramagnetically shifted peaks corresponding to the Fe^{II} complex **1**. For analysis by Mössbauer spectroscopy, complex **2** was enriched in ^{57}Fe (95.93%) and 2-MeTHF was employed in place of CD_3CN for product analysis because 2-MeTHF gives a better resolved, sharp doublet for the Mössbauer spectrum of **1**. The Mössbauer spectrum (80 K) showed a sharp quadrupole doublet ($\delta = 1.14$, $|\Delta E_Q| = 2.24$ mm s^{-1}, 90% of the fit) corresponding to **1**.

Reaction between 2 and (*p*-OMe-$C_6H_4)_3$C•. Crystalline **2** (2.0 mg, 0.002 mmol) was dissolved in THF (600 μL). The radical (*p*-OMe-$C_6H_4)_3$C• was freshly prepared according to a literature procedure,[3] as follows: an amount of (*p*-OMe-$C_6H_4)_3$CCl (20.8 mg, 0.056 mmol) was dissolved in toluene-d_8 (1 mL) and excess Cu powder was added, and the heterogenous mixture was heated in the dark for 1 h at 75 ºC. The resulting dark red solution was cooled to 23 °C, filtered through Celite, and an aliquot of this solution (100 μL, 1 equiv) was added to **2**. The reaction was stirred for 2 h, and then the solvent was removed under vacuum to give an orange residue, which was dissolved in CD_3CN and analyzed by ^{1}H NMR spectroscopy. The ^{1}H NMR spectrum showed complete disappearance of the broad, paramagnetically shifted peaks for the Fe^{III} complex **2**, and appearance of the relatively sharp, paramagnetically shifted peaks corresponding to the Fe^{II} complex **1**. For analysis by Mössbauer spectroscopy, complex **2** was enriched in ^{57}Fe (95.93%) and 2-MeTHF was employed in place of CD_3CN for product analysis because 2-MeTHF gives a better

resolved, sharp doublet for the Mössbauer spectrum of **1**. The Mössbauer spectrum (80 K) showed a sharp quadrupole doublet ($\delta = 1.14$, $|\Delta E_Q| = 2.24$ mm s^{-1}, 90% of the fit) corresponding to **1**.

Quantification of the alcohol product Ph_3COH in the reaction of 2 with Ph_3C•. Crystalline **2** (2.5 mg, 0.003 mmol) was dissolved in THF-d_8 (500 μL) to give a final solution of 5.08 mM in **2**. Excess $(Ph_3C)_2$ (12.4 mg, 0.025 mmol, 10 equiv) was added to the solution of **2** in THF-d_8 and stirred in the dark for 4 h. The ^{1}H NMR standard trimethylphenylsilane (TMPS) (10 μL, 7.01 mM) was added, and the reaction mixture was transferred into an NMR tube. Analysis by ^{1}H NMR spectroscopy revealed a peak at 5.51 ppm which can be assigned to the OH proton in Ph_3COH based on comparison with an authentic sample. Integration of this peak and comparison with the TMPS standard gave a final yield of the alcohol product. Average yield (3 runs) for Ph_3COH = 84% (±3).

Quantification of the alcohol product (p-OMe-$C_6H_4)_3COH$ in the reaction of 2 with (p-OMe-$C_6H_4)_3C$•. ^{1}H NMR spectroscopy. Crystalline **2** (1.7 mg, 0.002 mmol) was dissolved in THF-d_8 (500 μL) to give a final solution of 4.11 mM in **2**. The radical (p-OMe-$C_6H_4)_3C$• was freshly prepared according to a literature procedure,[3] as follows: an amount of (p-OMe-$C_6H_4)_3CCl$ (20.8 mg, 0.056 mmol) was dissolved in toluene-d_8 (1 mL) and excess Cu powder was added, and the heterogenous mixture was heated in the dark for 1 h at 75 °C. The resulting dark red solution was cooled to 23 °C, filtered through Celite, and an aliquot of this solution (100 μL, 1 equiv) was added to **2.** The reaction mixture was stirred for 2 h in the dark, and the ^{1}H NMR standard trimethylphenylsilane (TMPS) (3.94 mM) was added and the mixture was transferred to an NMR tube. Analysis by ^{1}H NMR spectroscopy revealed a peak at 5.24 ppm which can be assigned to the OH proton in (p-OMe-$C_6H_4)_3COH$ based on comparison with an authentic sample. Integration of this peak and comparison with the TMPS standard gave a final yield of the alcohol product. Average yield (3 runs) for (p-OMe-$C_6H_4)_3COH$ = 87% (±2).

DFT computational studies. All calculations were performed with the ORCA-3.0.2 program package.[7] Initial geometries were obtained from X-ray crystallographic models. Optimized geometries were calculated using the BP86 functional.[8] The 6-311g* basis set[9] was used for all Fe, N, O, S and F atoms and the 6-31g* basis set[10] was used for all C and H atoms. Frequency calculations at the same level of theory confirmed that all optimizations had converged to true minima on the potential energy surface (i.e., no imaginary frequencies). The optimized structures using the BP86 functional were used for Mössbauer parameter calculations for **1** and **2** because of the close match between the X-ray crystallographic and calculated metrics for **1** and **2.** Mössbauer parameters were computed using the B3LYP functional[11] and basis sets CP(PPP)[12] for Fe and def2-TZVP[13] for all other atoms. The angular integration grid was set to Grid4 (NoFinalGrid), with increased radial accuracy for the Fe atom (IntAcc 7). A continuum solvation model was included (COSMO), with a solvent of intermediate dielectric (methanol). The isomer shift was obtained from the electron density at the Fe nucleus, using a linear fit function previously reported: $\delta = \alpha(\rho(0) - c) + \beta$. For the methodology described here, $\alpha = -0.424$ au^3 mm s^{-1}, $\beta = 7.55$ mm s^{-1}, and $c = 11800$ au^{-3}.[14]

Single crystal X-ray crystallography. All reflection intensities were measured at 110(2) K using a SuperNova diffractometer (equipped with Atlas detector) with Mo *K*α radiation (λ = 0.71073 Å) under the program CrysAlisPro (Version CrysAlisPro 1.171.39.29c, Rigaku OD, 2017). The same program was used to refine the cell dimensions and for data reduction. The structure was solved with the program SHELXS-2014/7 (Sheldrick, 2015) and was refined on F^2 with SHELXL-2014/7 (Sheldrick, 2015). Numerical absorption correction based on gaussian integration over a multifaceted crystal model was applied using CrysAlisPro. The temperature of the data collection was controlled using the system Cryojet (manufactured by Oxford Instruments). The H atoms were

placed at calculated positions (unless otherwise specified) using the instructions AFIX 23, AFIX 43 or AFIX 137 with isotropic displacement parameters having values 1.2 or 1.5 *U*eq of the attached C atoms. The H atoms attached to N1, N5 and O2 (in complex **2**) were found from difference Fourier maps, and their coordinates were refined pseudo-freely using the DFIX restraints to keep the N–H and O–H bond distances within acceptable ranges.

Additional notes for the refinement of 1. The coordinated triflate anion is found to be disordered over two orientations, and the occupancy factor of the major component of the disorder refines to 0.8851(18). The crystal was pseudo-merohedrally twinned with two twin components. The twin relationship corresponds to a twofold axis along the **b** direction, and the BASF scale factor refines to 0.0635(9).

Additional notes for the refinement of 2. The coordinated triflate anion is found to be disordered over two orientations, and the occupancy factor of the major component of the disorder refines to 0.60(2). The asymmetric unit contains one disordered lattice toluene solvent molecule which is located at a site of inversion symmetry. Its occupancy factor has been constrained to 0.5.

D. Supporting Schemes:

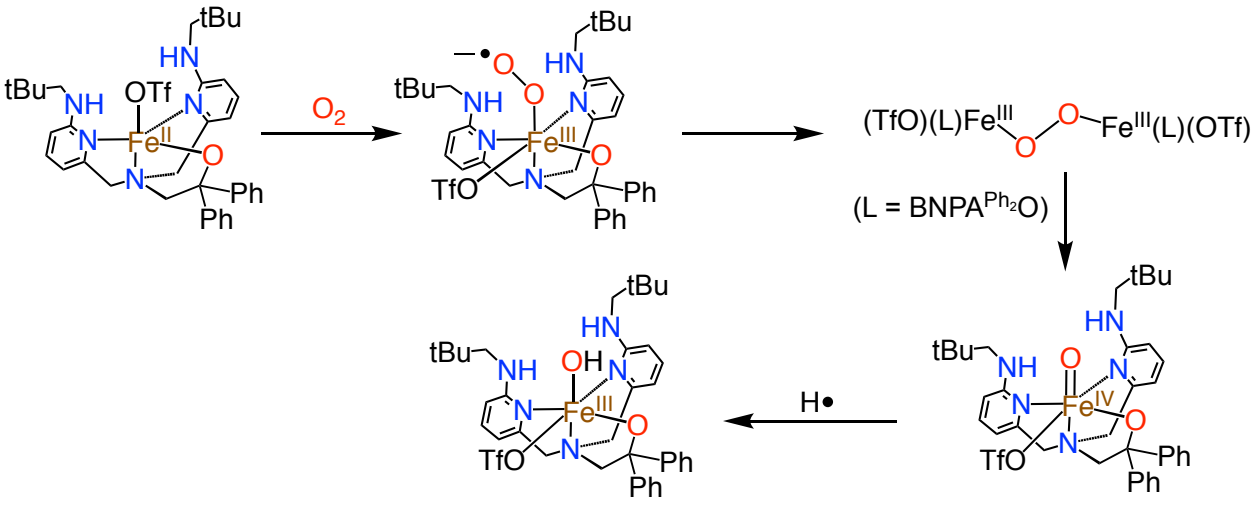

Scheme S1. Proposed mechanism for the formation of **2.**

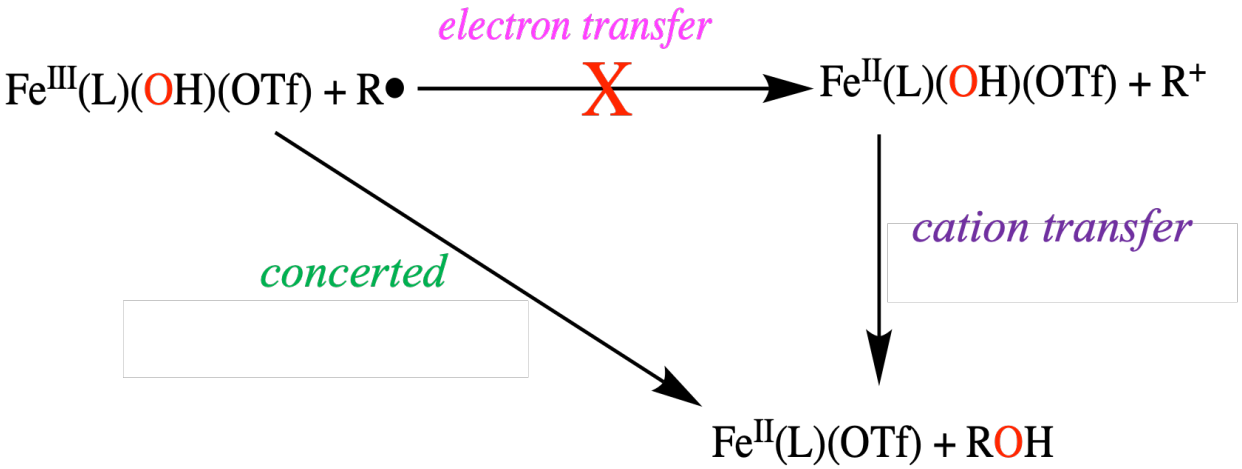

Scheme S2. Concerted versus stepwise pathway of radical hydroxylation.

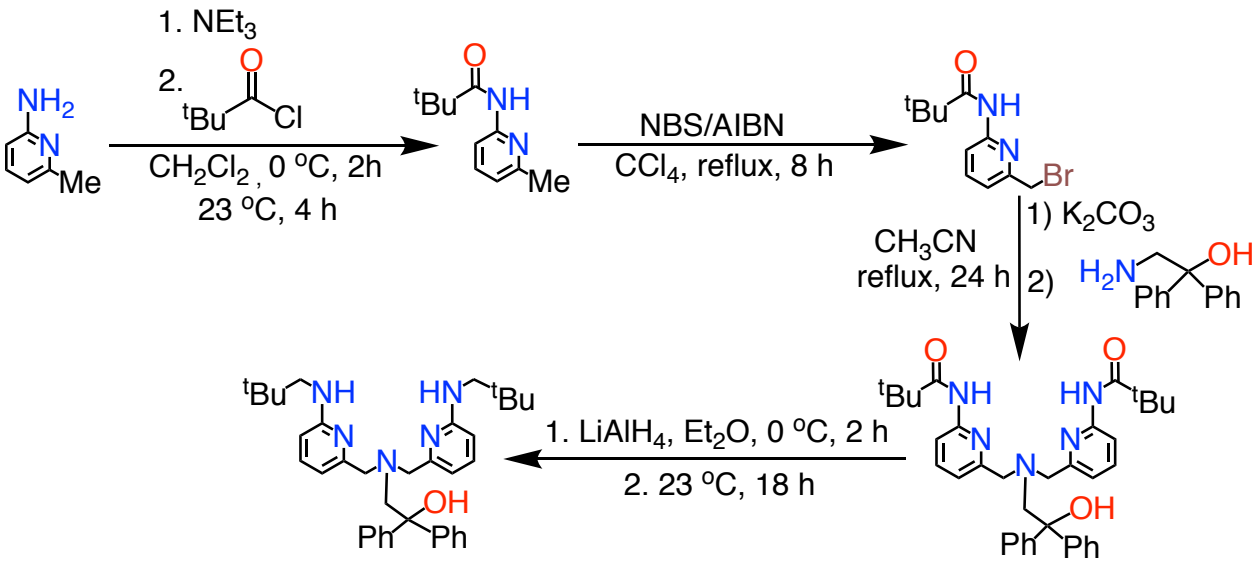

Scheme S3. Synthesis of BNPA^{Ph_2}OH

E. Experimental Tables. Table S1. Comparison of metrical parameters obtained from X-ray crystallography and DFT calculation for **1**.

	Bond lengths (Å) and bond angles (°) by XRD	Bond lengths (Å) and bond angles (°) from DFT
Bond Lengths		
Fe1–N2	2.153(2)	2.215
Fe1–N3	2.173(2)	2.157
Fe1–N4	2.174(2)	2.164
Fe1–O1	1.900(1)	1.886
Fe1–O2	2.160(2)	2.095
N1–O2	3.026(2)	3.031
N5–O2	3.116(2)	2.974
Bond Angles		
N2–Fe1–N3	77.45(6)	77.09
N2–Fe1–N4	99.37(6)	103.48
N3–Fe1–N4	78.49(6)	78.03
N2–Fe1–O1	114.71(6)	107.74
N3–Fe1–O1	82.67(6)	80.93
N4–Fe1–O1	136.05(6)	136.77
O1–Fe1–O2	95.61(6)	102.70
O2–Fe1–N2	101.59(6)	98.19
O2–Fe1–N3	176.07(6)	175.28

O2–Fe1–N4	105.14(7)	103.47
N1–H1–O2	161(2)	157.39
N5–H5–O2	166(2)	159.59

Table S2. Comparison of metrical parameters obtained from X-ray crystallography and DFT calculation for **2**.

	Bond lengths (Å) and bond angles (°) by XRD	Bond lengths (Å) and bond angle (°) by DFT
Bond lengths		
Fe1–N2	2.160(2)	2.193
Fe1–N3	2.166(2)	2.228
Fe1–N4	2.159(2)	2.170
Fe1–O1	1.856(1)	1.882
Fe1–O3	2.202(2)	2.204
Fe1–O2	1.880(1)	1.890
N1–O2	2.857(2)	2.864
N5–O2	2.831(3)	2.843
Bond angles		
N2–Fe1–N3	77.74(7)	79.21
N2–Fe1–N4	154.51(7)	153.96
N3–Fe1–N4	78.04(6)	76.79
N2–Fe1–O1	92.85(6)	92.09
N3–Fe1–O1	85.00(6)	81.88
N4–Fe1–O1	92.85(6)	94.37
O1–Fe1–O3	166.51(6)	164.02
O3–Fe1–N1	83.87(6)	83.79

O3–Fe1–N2	81.52(6)	82.24
O3–Fe1–N3	81.52(7)	83.11
O2–Fe1–N1	101.82(6)	103.13
O2–Fe1–N2	173.18(7)	172.76
O2–Fe1–N3	101.61(6)	99.55
O2–Fe1–O2	91.66(6)	91.20
O2–Fe1–O1	101.82(6)	104.75
N1–H1–O2	166(3)	162.05
N5–H5–O2	162(2)	160.53
O5–H2–O2	160(3)	159.94

Table S3. Optimized coordinates for **1**.

Fe	12.08460687662624	10.97141457943490	4.16211247674054
C	12.13045417436649	14.01662742945591	8.32011780710406
H	11.62657230896040	13.66799936991964	7.40474114961570
H	11.59135995358856	14.92331004202481	8.64562772299543
H	12.01151492843013	13.24753353061659	9.10624365837826
C	13.78720058436429	15.36521609422666	6.94240405128356
H	13.41866013734984	14.96773296577661	5.98459873912589
H	14.84885475117238	15.64651607876196	6.81511830685744
H	13.21149655117404	16.28209697667868	7.15361878985431
C	14.21912106531051	14.93091635248593	9.38510569726620
H	13.70919976899047	15.87479581242119	9.64463627259410
H	15.29687528328104	15.15080209640981	9.27458249481862
H	14.09522577836036	14.23727501009229	10.23744387554986
C	13.62145094796272	14.34245542816878	8.08605022907039
C	14.42095401655757	13.05558718537453	7.77470098317269
H	15.48735750169183	13.32924020284779	7.63130672756749
H	14.37352904822088	12.38587035186634	8.65915658501545
C	14.47668757920215	11.11118054769882	6.25230428543173
C	15.60798669862219	10.57303588804996	6.93922634634274
C	16.08097852643495	9.31736384549796	6.58855190500518
C	15.44008411314629	8.59038193339306	5.56847528231004

H	15.76936016699931	7.58713078359612	5.28656366953672
C	14.35987696174749	9.18492435438930	4.91553396918018
C	13.66746221746397	8.45987687759492	3.77355283904958
H	14.12838650708626	8.77214906778209	2.81844088883036
H	13.82900998918821	7.36505061238366	3.86539946737775
C	11.66683213321279	8.75677883707909	2.36141496735037
C	12.35665522232138	9.77626949024291	1.47374203670394
C	12.61827916733452	9.50706538124716	0.13281808671370
H	12.33014705094848	8.54610434005682	-0.30094462209029
C	13.26378703986148	10.50120081641255	-0.62972349223411
H	13.48426598158090	10.33132323949236	-1.68855625187127
C	13.64722005653352	11.69071169637360	-0.02780037186218
H	14.18221735136277	12.45252010508951	-0.59649908392972
C	13.36027106586201	11.90429267855812	1.35307679721657
C	14.27543098780652	14.25335797626067	1.42598863010577
H	13.71841598631905	15.08722794463371	1.88798571239858
H	14.03610680197773	14.27607571615040	0.34731289357609
C	15.80241081328854	14.47170523497208	1.63130102068953
C	16.61489433413825	13.36948548172823	0.92245091734393
H	16.33532079743527	12.36554067338061	1.28754277515041
H	17.69710605926308	13.50393510006802	1.10498929972359
H	16.45848507345826	13.39265498046467	-0.17272388274466
C	16.15155166637392	15.84875530386380	1.02642622462327

H	15.91237361797325	15.89009551582250	-0.05258066988694
H	17.22963431406145	16.06273708964543	1.13796816738729
H	15.59408829595012	16.65988279316008	1.52819916015859
C	16.13115244549084	14.47288880039883	3.13899657711763
H	15.55761673444815	15.25237250695148	3.67155667444307
H	17.20628311471795	14.67152898634351	3.30184889154292
H	15.89448213279035	13.49953115003847	3.60282807490545
C	11.45104776867188	8.14417317510813	4.78002284871571
H	12.11166791204294	8.08465342003109	5.66015225466949
H	11.18744656497886	7.10532682337365	4.49790088544169
C	10.21284451927886	9.01638889709909	5.20146590605509
C	9.84457166733847	8.60646520268132	6.65529633165033
C	9.97492865423978	9.55286739253729	7.68704433599243
H	10.30516852121924	10.55977890888062	7.41947441893479
C	9.67689572872141	9.20777316317920	9.01453099220552
H	9.77464868991649	9.96097962754992	9.80465168713850
C	9.25258224230656	7.90846129444547	9.33161282963486
H	9.01667482168777	7.63951670978053	10.36713486640201
C	9.12126616376627	6.95725563295803	8.30764138005033
H	8.78174969967968	5.94173363769135	8.54047343300970
C	9.41008987382152	7.30561125735018	6.97968157771334
H	9.27391009052375	6.55816855920477	6.19059480027561
C	8.96414519388723	8.78014581659129	4.30634849623872

C	8.63767332224361	7.54042225239892	3.71596951190969
H	9.29665596642604	6.67332467790183	3.83718291226610
C	7.46627697211444	7.38717435256949	2.95539049290707
H	7.23949235121594	6.41532925256828	2.50304529776887
C	6.59439071031949	8.47032380520826	2.77433827761307
H	5.68022405906926	8.35130489663082	2.18279975848429
C	6.90565326129240	9.70700126297756	3.36238376954276
H	6.23275744650467	10.56213748050302	3.23200623761130
C	8.07640697972555	9.85793189339257	4.11814804543402
H	8.32730674613695	10.81502908667490	4.57789971734009
N	13.95432821037974	12.31600001464893	6.60039078591338
H	13.13749443560522	12.64860419366539	6.07103187860835
N	13.88043163102366	10.42251432436486	5.22346760041502
N	12.23819569543187	8.80685877588040	3.71629696374180
N	12.69800923691348	10.94755652213381	2.08712225043623
N	13.73867327969098	13.02851613564698	2.01989678805677
H	13.32416379903663	13.13507475188804	2.95454327927170
O	10.61225927714263	10.35557230955185	5.16700173106886
H	16.94212281339854	8.89277964795442	7.11487156003738
H	16.08614291421474	11.14533838761014	7.73526077713059
H	11.73649539478485	7.74612736340030	1.90206624394456
H	10.59276270564360	8.99842417856791	2.45482265675287
O	11.98112953561511	13.04817941827179	4.41906769564366

S	11.10547617912050	14.30784015203369	4.16574081672113
O	10.68408521129281	14.95713389566965	5.41701742056707
O	11.67662590311752	15.13732569588998	3.08466344518491
C	9.50608871060731	13.58038117793947	3.42383063108563
F	8.88481743597513	14.51685688506198	2.68849941302574
F	9.79286776631401	12.52690663260947	2.62437938198691
F	8.67465925675338	13.17606580254029	4.39679486279628

Table S4. Optimized coordinates for **2**

Fe	3.43798831863180	0.80127678363392	5.08380621039242
C	7.37279085000397	2.89498806602663	7.55438700628255
H	7.63755286750824	3.78985325382124	6.96196436872119
H	6.92390183518453	2.15344883599530	6.87215382294304
H	8.30923081501883	2.46264227934679	7.94864785356303
C	6.04955905929684	1.98492987539642	9.51287980939132
H	6.95619885247335	1.53625910768502	9.95670379354382
H	5.58159305164879	1.21646415337045	8.87409950583447
H	5.34986400489516	2.21861423295395	10.33545260365422
C	7.11633559604906	4.26208870744830	9.65807560331881
H	6.45792371281921	4.55222877493286	10.49728650111871
H	7.41052559714497	5.18277139476709	9.12160595732226
H	8.03118366497930	3.81857998782694	10.08816327652102
C	6.42025846006670	3.25514230754625	8.71563057599077
C	5.14626171989438	3.95685292525928	8.17767091577925
H	4.48574999321876	4.20628159868573	9.03613103478344
H	5.44571740774884	4.91732193163372	7.71039596195737
C	3.31196075642686	3.62861336593193	6.54856021188684
C	2.78673730604377	4.93916752604533	6.76775951193611
C	1.67248197604701	5.35105796274800	6.05077866073582
C	1.06855605110161	4.48337813843646	5.11881532792754

H	0.19339252624404	4.78592819166225	4.53815361274928
C	1.61546847062991	3.20938464479459	4.96547722314011
C	0.99423870712851	2.18227391398999	4.03599943834106
H	0.34365054154690	1.52406400819556	4.63617491960473
H	0.37717261700015	2.68396244956158	3.26276400119985
C	1.49218289767471	0.05583790810576	2.88727078601158
H	1.17640087105928	0.17644255764196	1.83185975097798
H	0.59035112240039	-0.18255481329486	3.47844281421798
C	2.43234241707960	-1.13210054476775	3.01863850739703
C	2.30335443213473	-2.22758908359312	2.16488541408659
H	1.58783953743519	-2.20536078381028	1.33865400770724
C	3.11770914648079	-3.34928827112135	2.40561421309885
C	4.02155010690424	-3.34214129794361	3.45874432987116
C	4.11337999503826	-2.18649182019054	4.29010181282922
C	5.87244542879470	-3.20502015099771	5.70218007535490
H	6.61783500938298	-3.36618504986493	4.89453614714566
H	5.28447792892041	-4.14130301367303	5.79020767204810
C	6.62290333436195	-2.97846250415929	7.03921754283115
C	7.46143977133150	-1.68257159582215	6.98899654348417
H	8.15290797063561	-1.68636606289201	6.12579799283900
H	8.07074464370210	-1.59077922475698	7.90672748984005
H	6.82947665530676	-0.77984356806949	6.92102136865785
C	7.57058283537893	-4.18526633387839	7.22480667420938

H	7.01084439289943	-5.13868729425435	7.24862620961712
H	8.12102512683455	-4.09681261295441	8.17792754766257
H	8.31607497820351	-4.24574840440057	6.40989757271669
C	5.62715033430767	-2.93075529939763	8.21682982366273
H	4.89530613290699	-2.11170147005216	8.11827286271030
H	6.16578462729087	-2.78540957512963	9.17085086239080
H	5.05840105749565	-3.87541426235707	8.29518462262064
C	2.87187978689264	2.11398700503278	2.46465231812108
H	2.77797295162396	3.16742214521784	2.76934623594802
H	2.45141582816912	2.03549491631368	1.44380294561425
C	4.40676321008669	1.77343322438367	2.52964758469167
C	5.16608410174876	3.06421969972643	2.11240003031406
C	5.89425043179285	3.78223129271187	3.07812820086895
H	5.93784092819579	3.38669990867669	4.09595596603373
C	6.55161573767274	4.97370369439677	2.73381620981418
H	7.12046782767248	5.51737861509294	3.49639548499277
C	6.48263831879195	5.46958061532538	1.42319617227743
H	6.99244646364835	6.40122659583231	1.15593126203942
C	5.75751779948356	4.75797894903902	0.45448433367488
H	5.70185508792147	5.12980047721025	-0.57475962266595
C	5.10904192709240	3.56181611632713	0.79541166961374
H	4.57387843928733	3.00351001184227	0.01985599073410
C	4.86246268903110	0.62860918817970	1.59017209754295

C	4.25879271003156	0.34880391988347	0.34864288986809
H	3.36693179923815	0.89639261822180	0.02422640506602
C	4.78306335782686	-0.63747245361534	-0.50355387097127
H	4.29423554991563	-0.83745018894678	-1.46327954770785
C	5.92295730781148	-1.36070483822552	-0.12869960978729
H	6.33401670540382	-2.12817275031499	-0.79349844117345
C	6.53172584988099	-1.09125963835141	1.10789389392537
H	7.42514427272204	-1.64775464131268	1.41171228165272
C	6.00730763704945	-0.10794535330617	1.95658976903583
H	6.47513609623521	0.10537477482244	2.92163712158107
N	4.41214370401082	3.16695410627322	7.19405263275413
H	4.62975082069009	2.15634159415119	7.07092998407110
N	2.70652297037015	2.78966747767221	5.65011092029251
N	2.04377312135593	1.32207116104004	3.42614049313572
N	3.30995872789092	-1.10082149060331	4.04779694394909
N	4.97898809579068	-2.11148008038391	5.33224917881120
H	4.96684755766002	-1.23732386318907	5.89388327853079
O	4.71032043821804	1.45883378925265	3.86326441884278
O	4.43197155212379	0.37958757390562	6.63443597271802
H	3.88431448761205	0.03821333585838	7.39223320160040
O	1.57379479494216	0.10766680885121	6.03398717620382
S	1.26715644228577	-0.64018660118218	7.32689728262144
C	0.00434615879389	0.52547610485547	8.12594482268536

O	2.42247099297494	-0.62396826777838	8.27322675114826
F	-0.45257033116959	0.00736924813771	9.27861477902857
F	-1.04355125654346	0.71738092671520	7.29436885569341
F	0.56345900218880	1.72620573364285	8.38477636311066
H	3.04563139179141	-4.23031419766044	1.75883798406677
H	4.66356728725722	-4.20318259855433	3.65081446186273
H	1.26600941909697	6.35510237736939	6.21029726858324
H	3.26053773311124	5.59960617447363	7.49621191410622
O	0.55713856160948	-1.91392506307272	7.13282719245147

Table S5. Calculated Mössbauer Parameters for Complexes **1** and **2**.

complex[a]	calculated isomer shift[b,c]	experimental isomer shift[b]	calculated quadrupole splitting[b]	experimental quadrupole splitting[b]
1	1.05	1.03	2.61	2.42
2	0.47	0.47	1.42	0.97

[a] See DFT computational section for details regarding geometry optimizations.

[b] mm s^{-1}.

[c] Electron density at the nucleus ($\rho(0)$) calculated using the B3LYP functional with a combination of the CP(PPP) basis set for Fe and def2-TZVP basis set for all other atoms and calibrated as described in the DFT computational section.

Table S6. Crystallographic data for 1.

	xs1658a
Crystal data	
Chemical formula	$C_{37}H_{46}F_3FeN_5O_4S$
M_r	769.70
Crystal system, space group	Triclinic, *P*-1
Temperature (K)	110
a, *b*, *c* (Å)	10.0166 (3), 10.6374 (4), 18.2471 (6)
α, β, γ (°)	80.928 (3), 79.036 (3), 79.746 (3)
V (Å^3)	1862.77 (11)
Z	2
Radiation type	Mo *K*α
μ (mm^{-1})	0.52
Crystal size (mm)	0.15 × 0.11 × 0.06
Data collection	
Diffractometer	SuperNova, Dual, Cu at zero, Atlas
Absorption correction	Gaussian *CrysAlis PRO* 1.171.39.29c (Rigaku Oxford Diffraction, 2017) Numerical absorption correction based on gaussian integration over a multifaceted crystal model Empirical absorption correction using spherical harmonics, implemented in SCALE3 ABSPACK scaling

	algorithm.
T_{min}, T_{max}	0.876, 1.000
No. of measured, independent and observed [$I > 2\sigma(I)$] reflections	28180, 9583, 6152
R_{int}	0.039
$(\sin \theta/\lambda)_{max}$ ($Å^{-1}$)	0.650
Refinement	
$R[F^2 > 2\sigma(F^2)]$, $wR(F^2)$, S	0.039, 0.073, 0.81
No. of reflections	9583
No. of parameters	510
No. of restraints	268
H-atom treatment	H atoms treated by a mixture of independent and constrained refinement
$\Delta\rho_{max}$, $\Delta\rho_{min}$ (e $Å^{-3}$)	0.59, -0.39

Table S7. Crystallographic data for 2.

	xs1707a
Crystal data	
Chemical formula	$2(C_{37}H_{47}F_3FeN_5O_5S)\cdot C_7H_8$
M_r	1665.54
Crystal system, space group	Monoclinic, $P2_1/c$
Temperature (K)	110
a, b, c (Å)	19.6283 (5), 10.3255 (4), 20.5481 (6)
β (°)	98.061 (2)
V (Å^3)	4123.4 (2)
Z	2
Radiation type	Mo $K\alpha$
μ (mm^{-1})	0.48
Crystal size (mm)	0.28 × 0.23 × 0.18
Data collection	
Diffractometer	SuperNova, Dual, Cu at zero, Atlas
Absorption correction	Gaussian *CrysAlis PRO* 1.171.39.29c (Rigaku Oxford Diffraction, 2017) Numerical absorption correction based on gaussian integration over a multifaceted crystal model Empirical absorption correction using spherical harmonics, implemented in SCALE3

	ABSPACK scaling algorithm.
T_{min}, T_{max}	0.594, 1.000
No. of measured, independent and observed [$I > 2\sigma(I)$] reflections	32503, 9476, 8245
R_{int}	0.026
$(\sin \theta/\lambda)_{max}$ ($Å^{-1}$)	0.650
Refinement	
$R[F^2 > 2\sigma(F^2)]$, $wR(F^2)$, S	0.044, 0.108, 1.09
No. of reflections	9476
No. of parameters	603
No. of restraints	312
H-atom treatment	H atoms treated by a mixture of independent and constrained refinement
$\Delta\rho_{max}$, $\Delta\rho_{min}$ (e $Å^{-3}$)	0.65, -0.54

Table S8. Comparison of reduction potentials of Fe^{III}/Fe^{II} couple for 2 with some reported nonheme $Fe^{III}(OH)$ complexes.

No.	complex	$E^{o}_{1/2}$ (vs Fc^{+}/Fc^{0}) in V	solvent
1	$[Fe^{III}(tnpa)(OH)(PhCO_2)]ClO_4$	-0.47[15]	CH_3CN
2	$[Fe^{III}(tnpa)(OH)(CH_3CO_2)]ClO_4$	-0.67[15]	CH_3CN
3	$[Fe^{III}(tnpa)(OH)(HCO_2)]ClO_4$	-0.48[15]	CH_3CN
4	$[N4Py^{2Np}Fe^{III}(OH)](OTf)_2$	0[16]	CH_3CN
5	$[N4Py^{2Ph}Fe^{III}(OH)](OTf)_2$	-0.21[16]	CH_3CN
6	$K[Fe^{III}(OH)(H_3buea)]$	-1.93[17]	DMF
7	$K[Fe^{III}(OH)(H_2\mathbf{2}^{iPr})]$	-1.89[17]	DMF
8	K[Fe^{III}(OH)(H**1**iPr)]	-1.94[17]	DMF
9	$Fe^{III}(BNPA^{Ph_2}O)(OH)(OTf)$ (**2**)	-0.69	CH_3CN

F. Supporting figures.

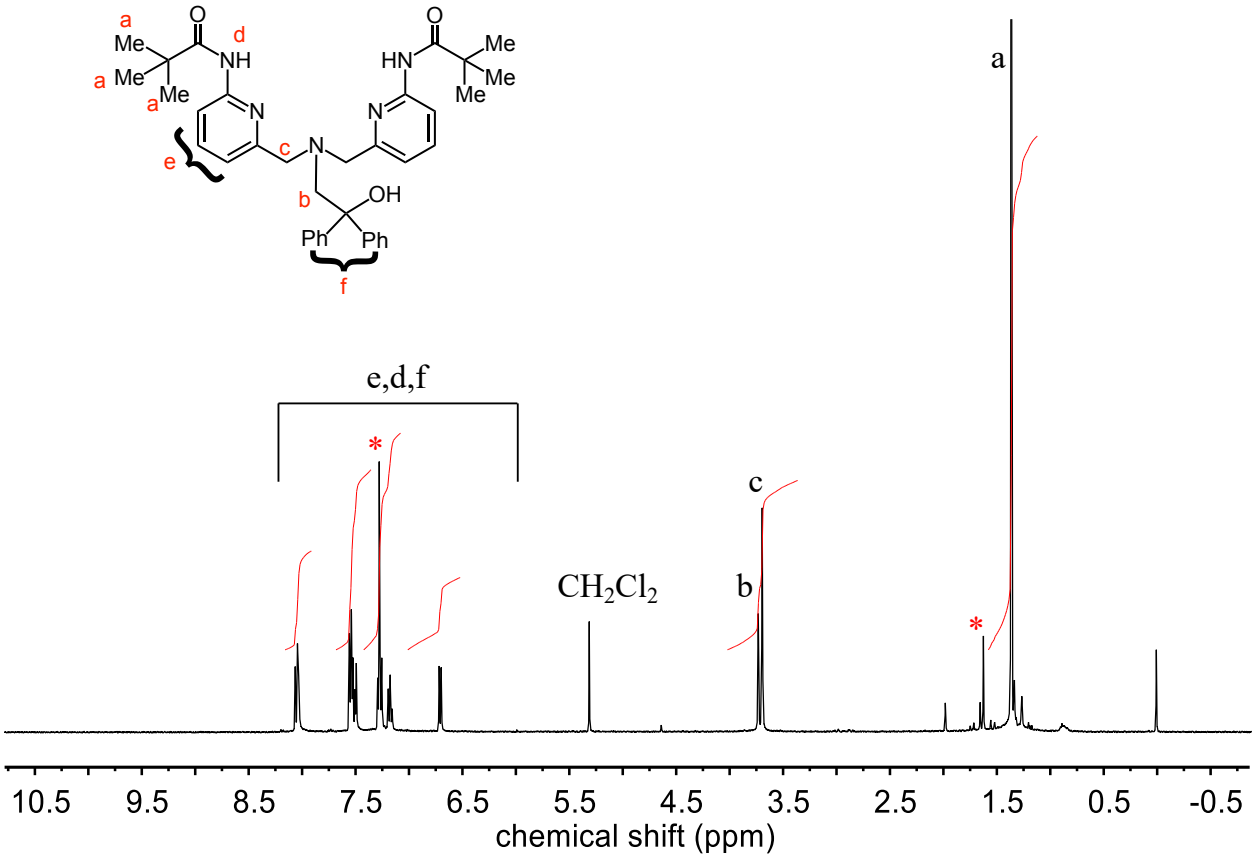

Figure S1. ^{1}H NMR spectrum of BPPA^{Ph2}OH in $CDCl_3$. Residual solvent peaks for $CHCl_3$ and H_2O are marked with an asterisk (*).

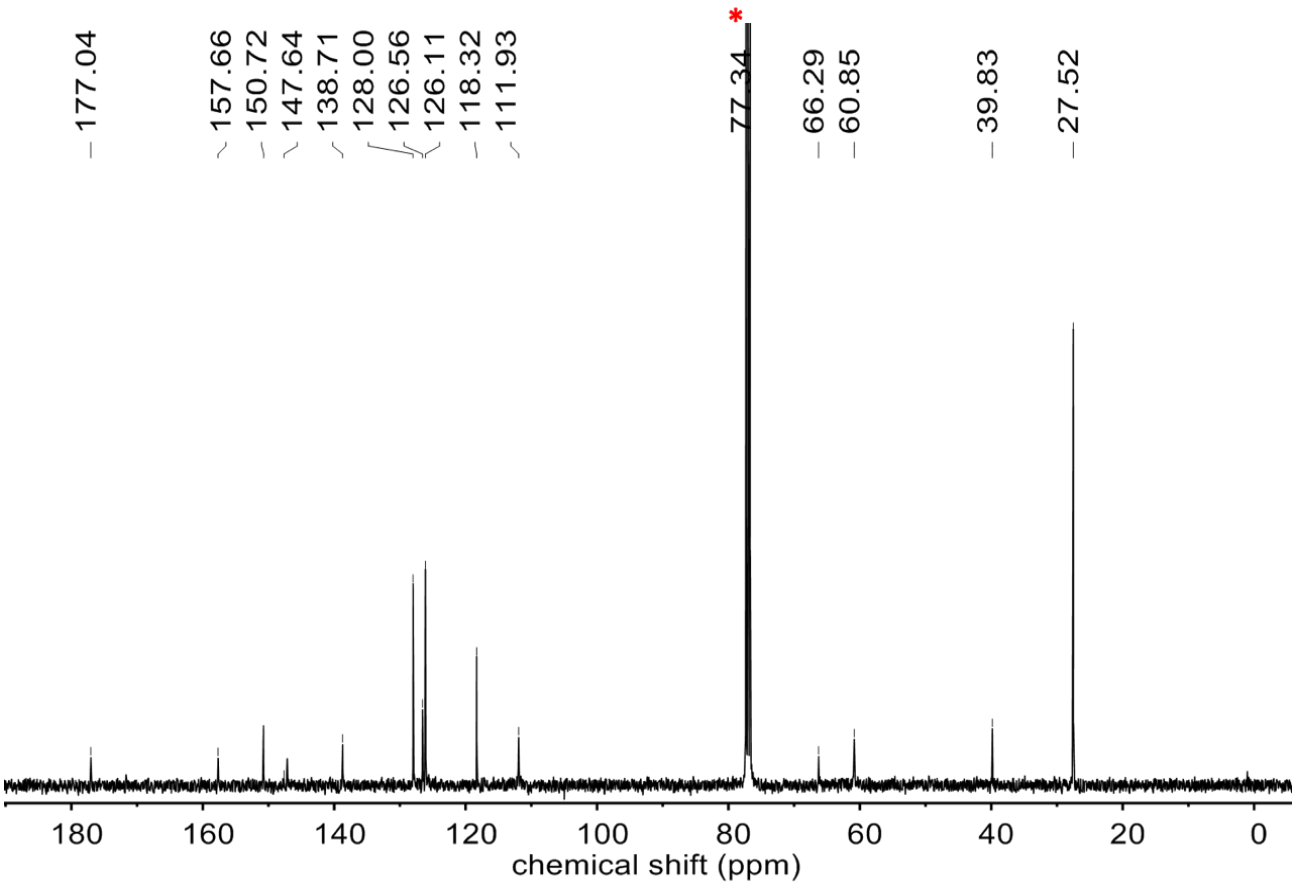

Figure S2. ^{13}C NMR spectrum of BPPA^{Ph_2}OH in $CDCl_3$. $CDCl_3$ peaks are marked with an asterisk (*).

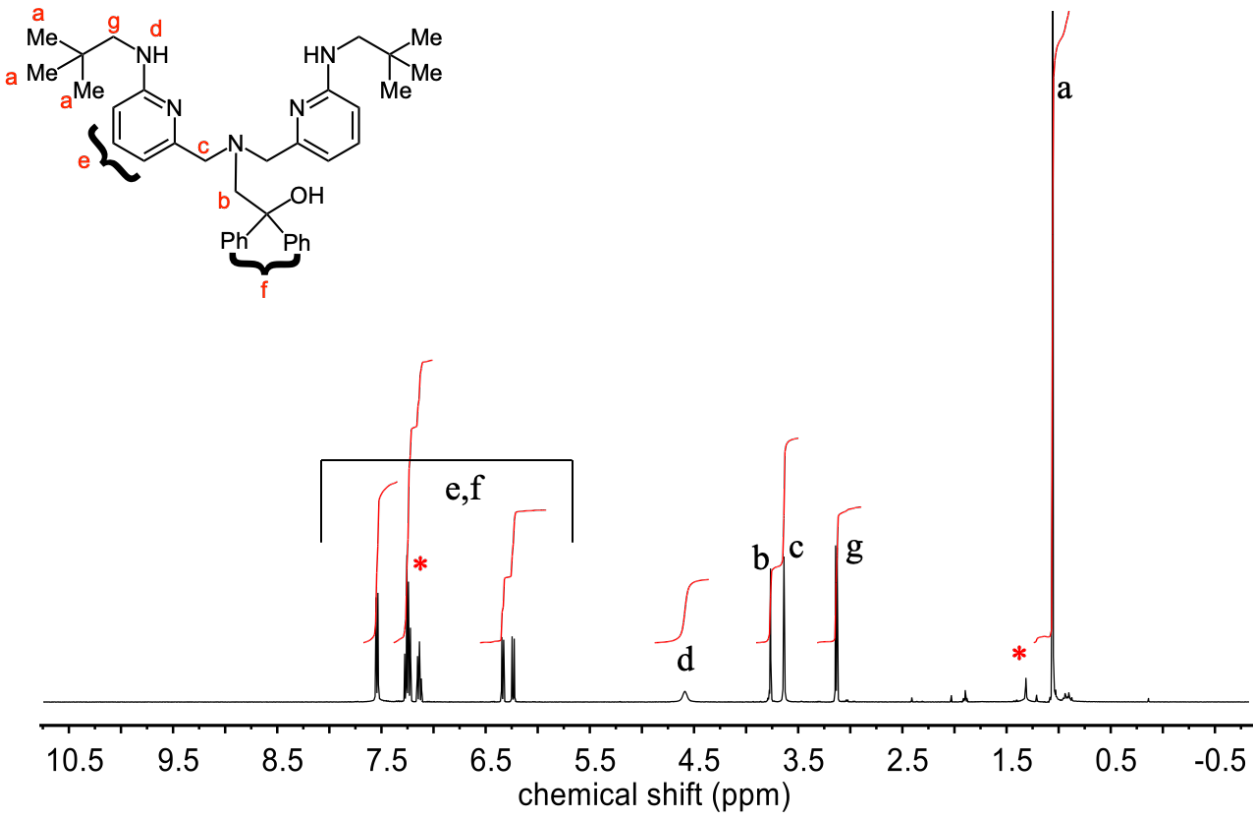

Figure S3. ^{1}H NMR spectrum of BNPA^{Ph_2}OH in $CDCl_3$. Residual solvent peaks for $CHCl_3$ and H_2O peaks are marked with an asterisk (*).

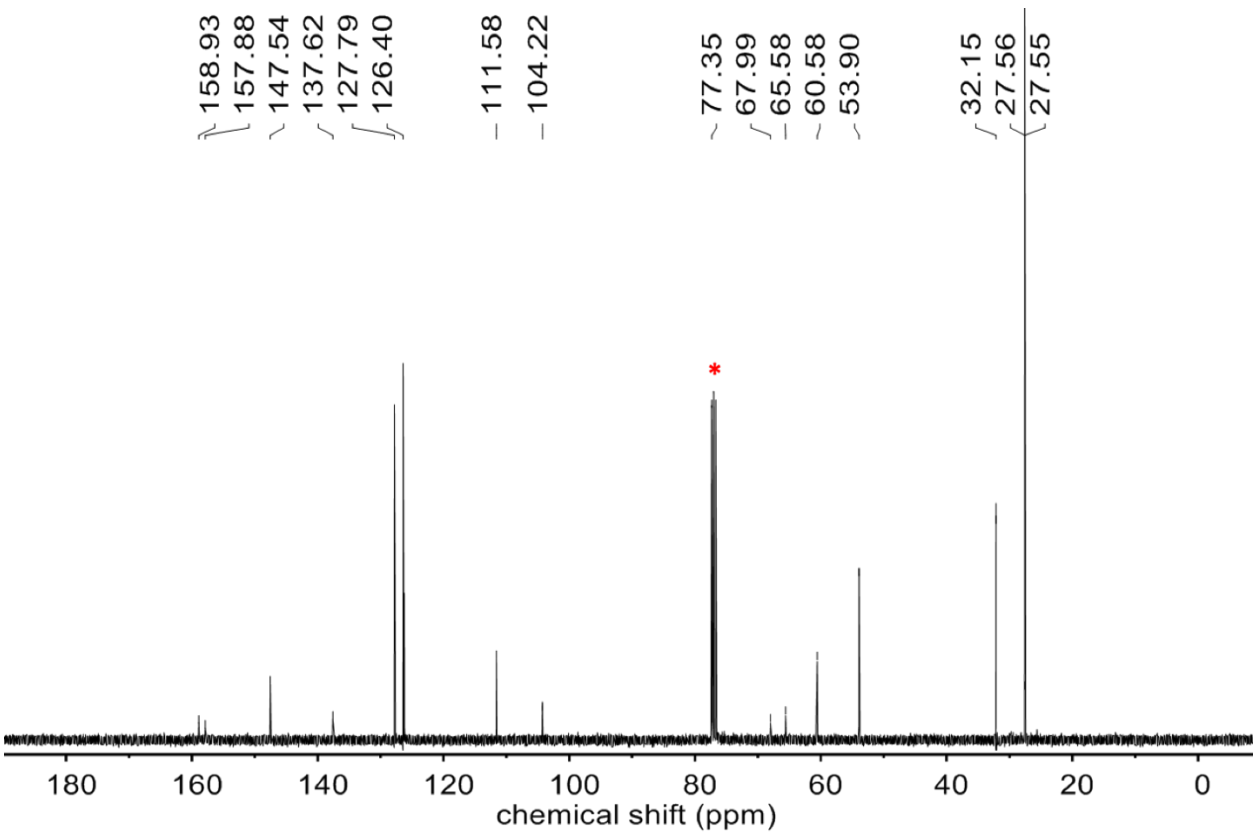

Figure S4. ^{13}C NMR spectrum of BNPA^{Ph_2}OH in $CDCl_3$. $CDCl_3$ peaks are marked with an asterisk (*).

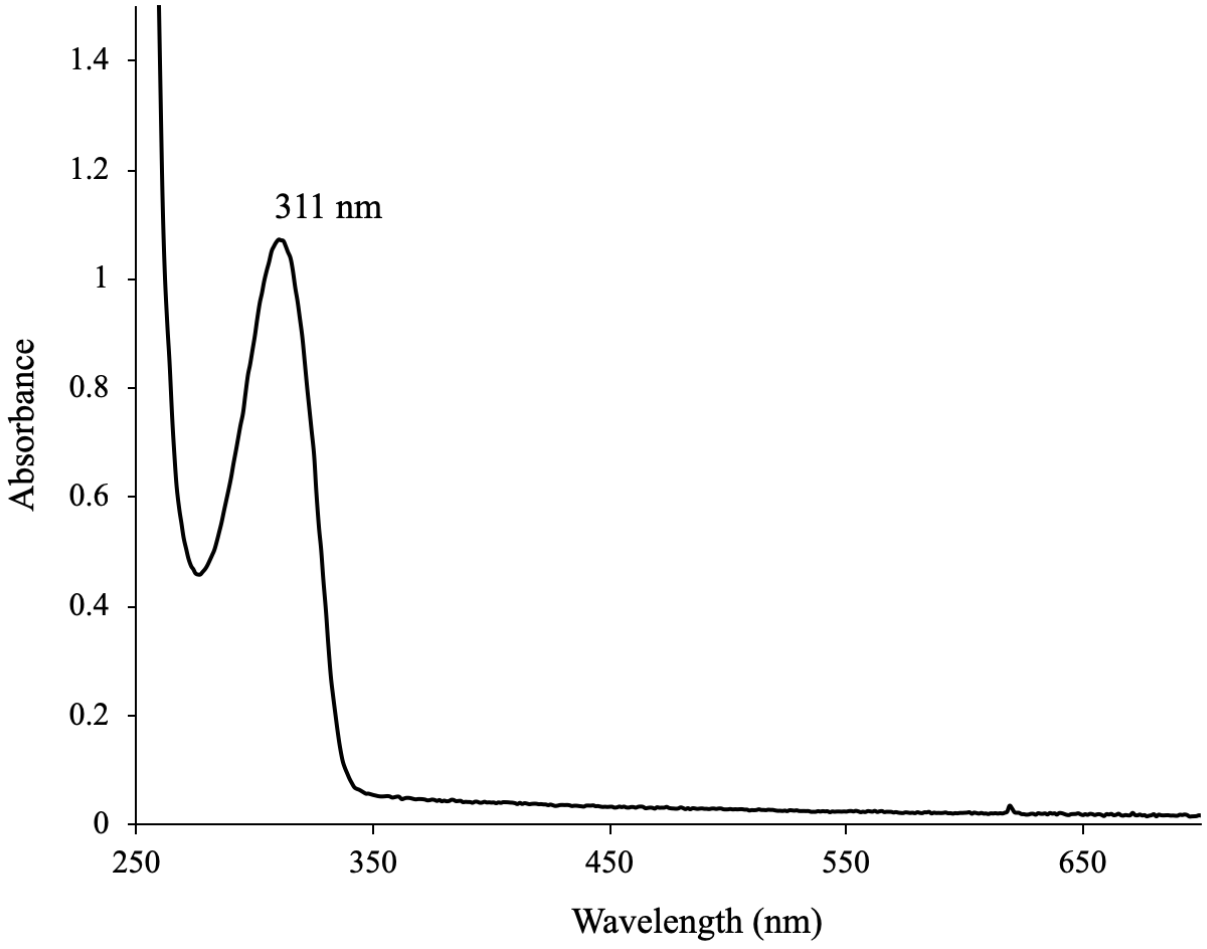

Figure S5. UV-vis spectrum of $BNPA^{Ph_2}OH$ in CH_3CN at 23 °C.

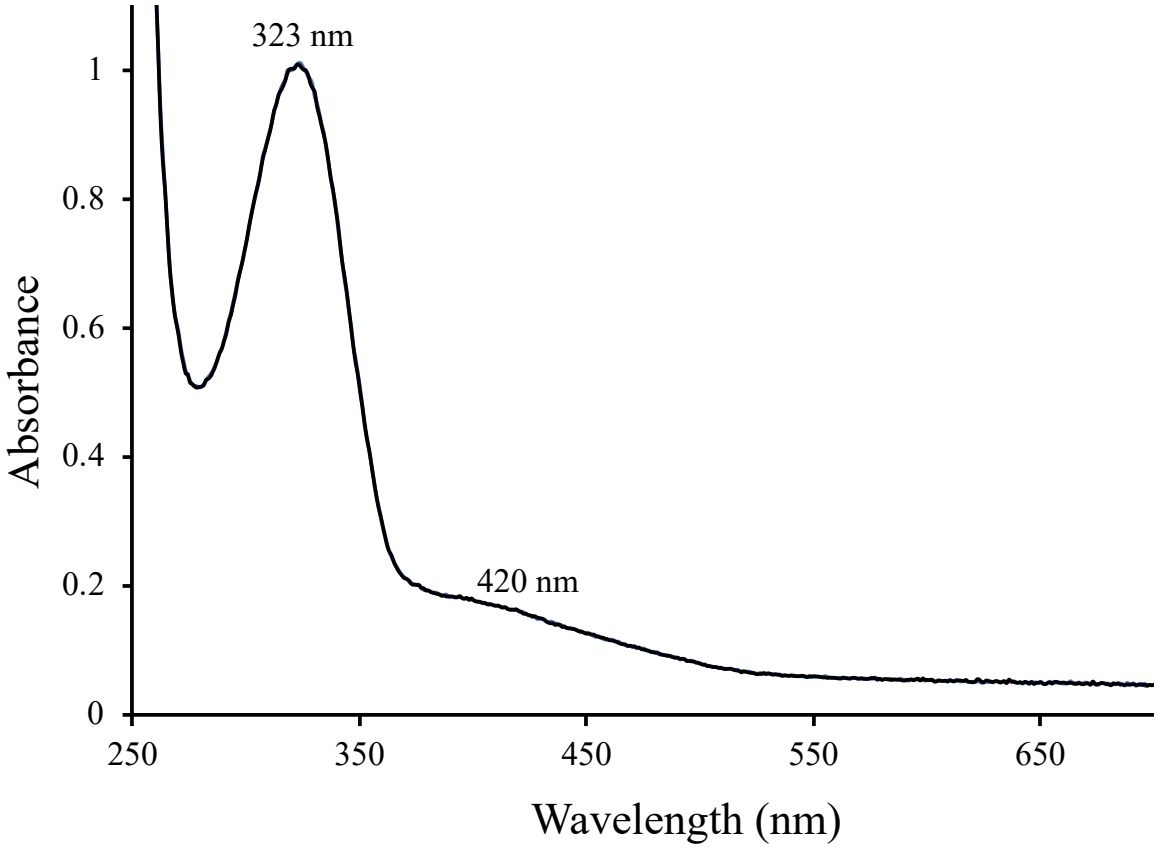

Figure S6. UV-vis spectrum of **1** (~80 μM) in CH_3CN at 23 ºC.

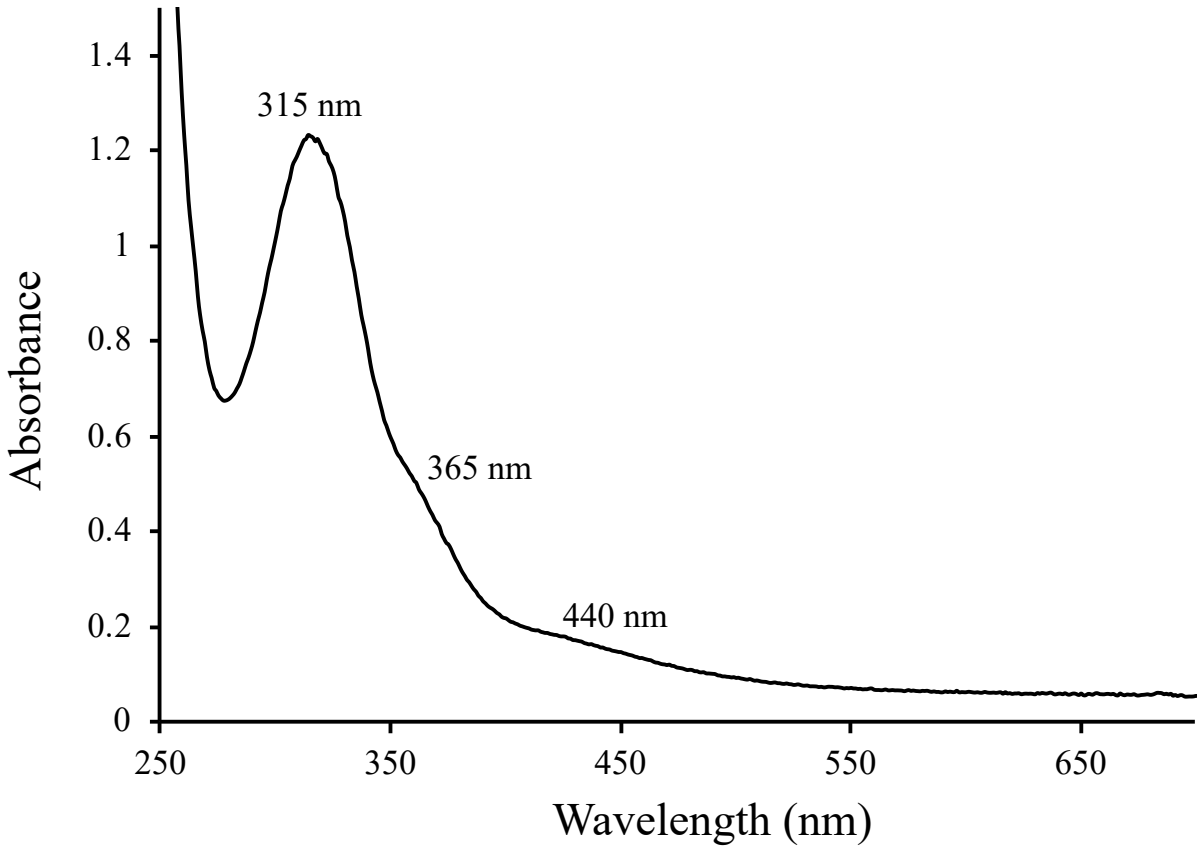

Figure S7. UV-vis spectrum of **2** (~80 μM) in CH_3CN at 23 °C.

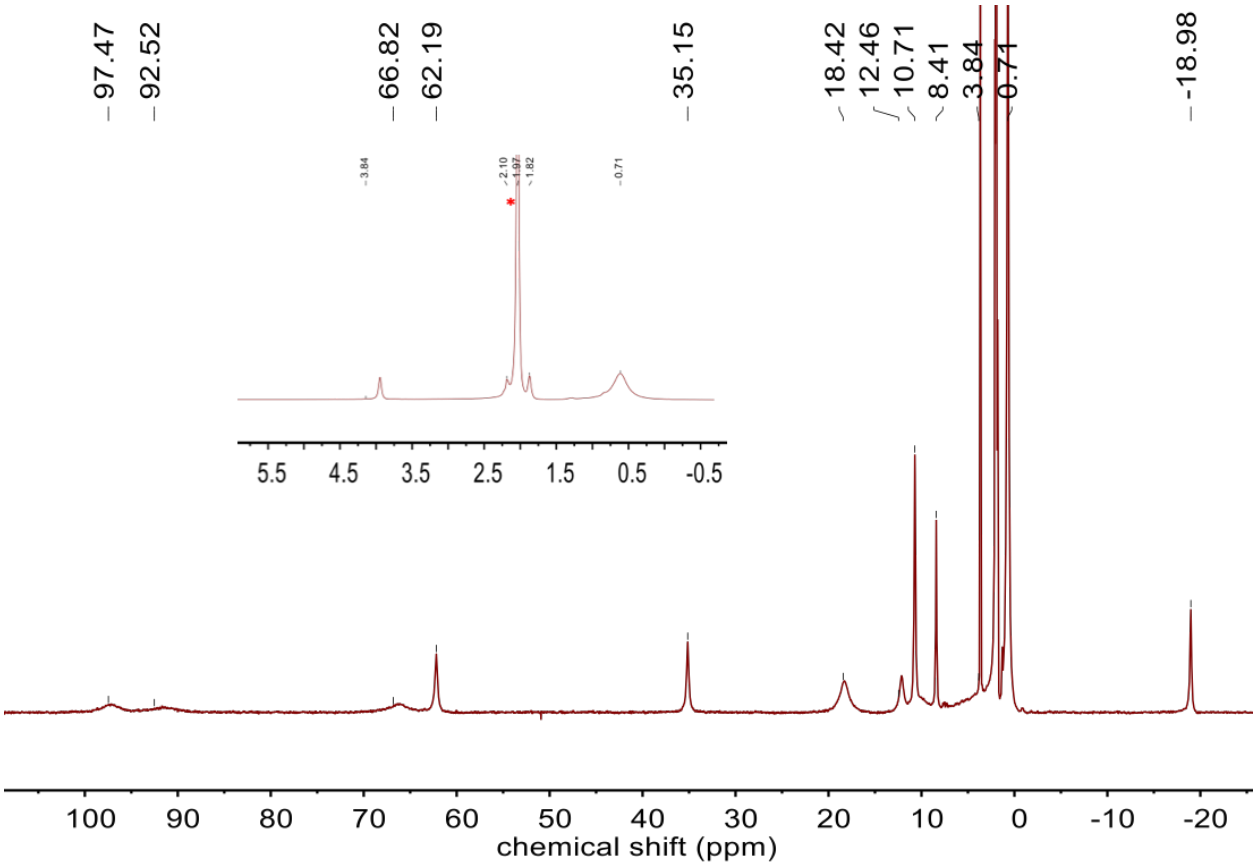

Figure S8. ^{1}H NMR spectrum of **1** in CD_3CN at 23 °C. Inset shows the expanded diamagnetic region. Residual solvent CH_3CN is marked with an asterisk (*).

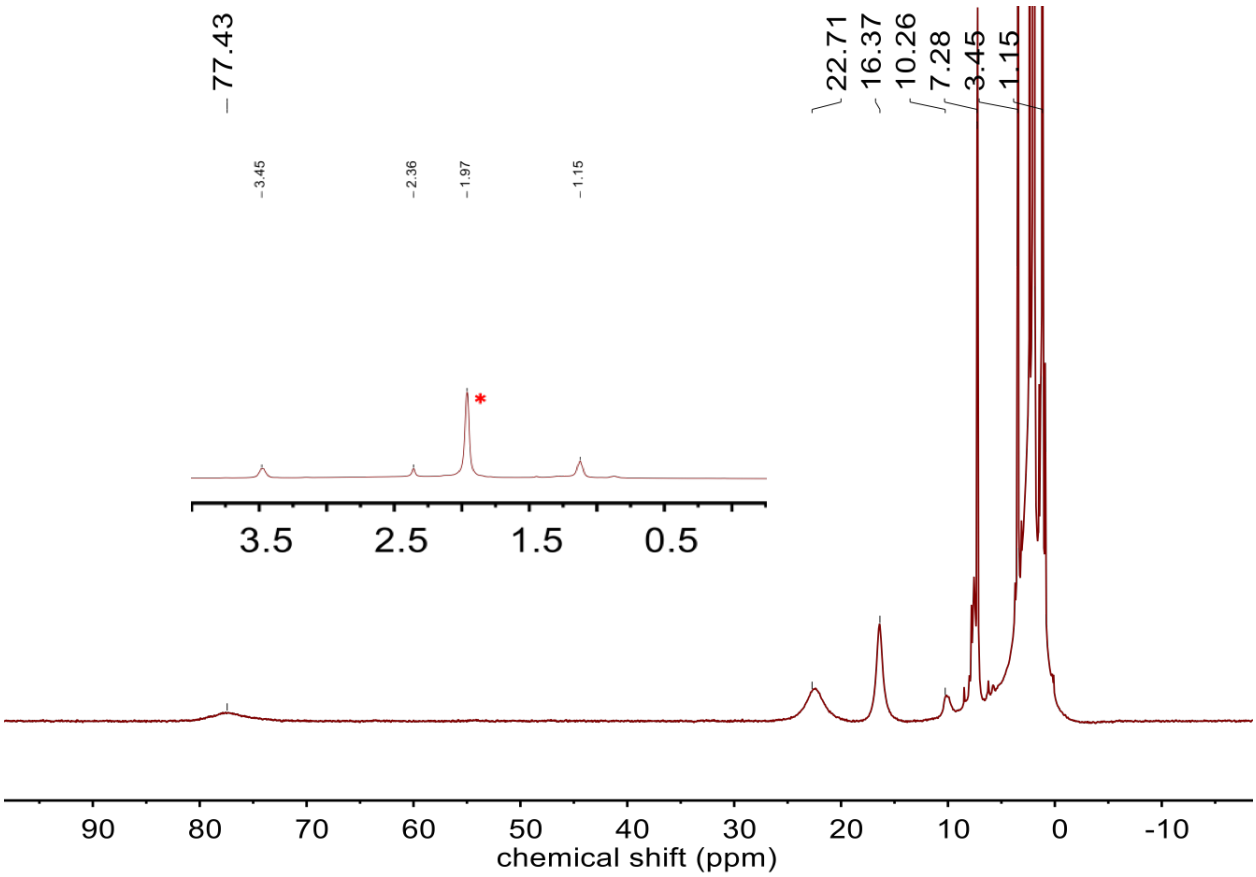

Figure S9. ^{1}H NMR spectrum of **2** in CD_3CN at 23 °C. Inset shows the expanded diamagnetic region. Residual solvent CH_3CN is marked with an asterisk (*).

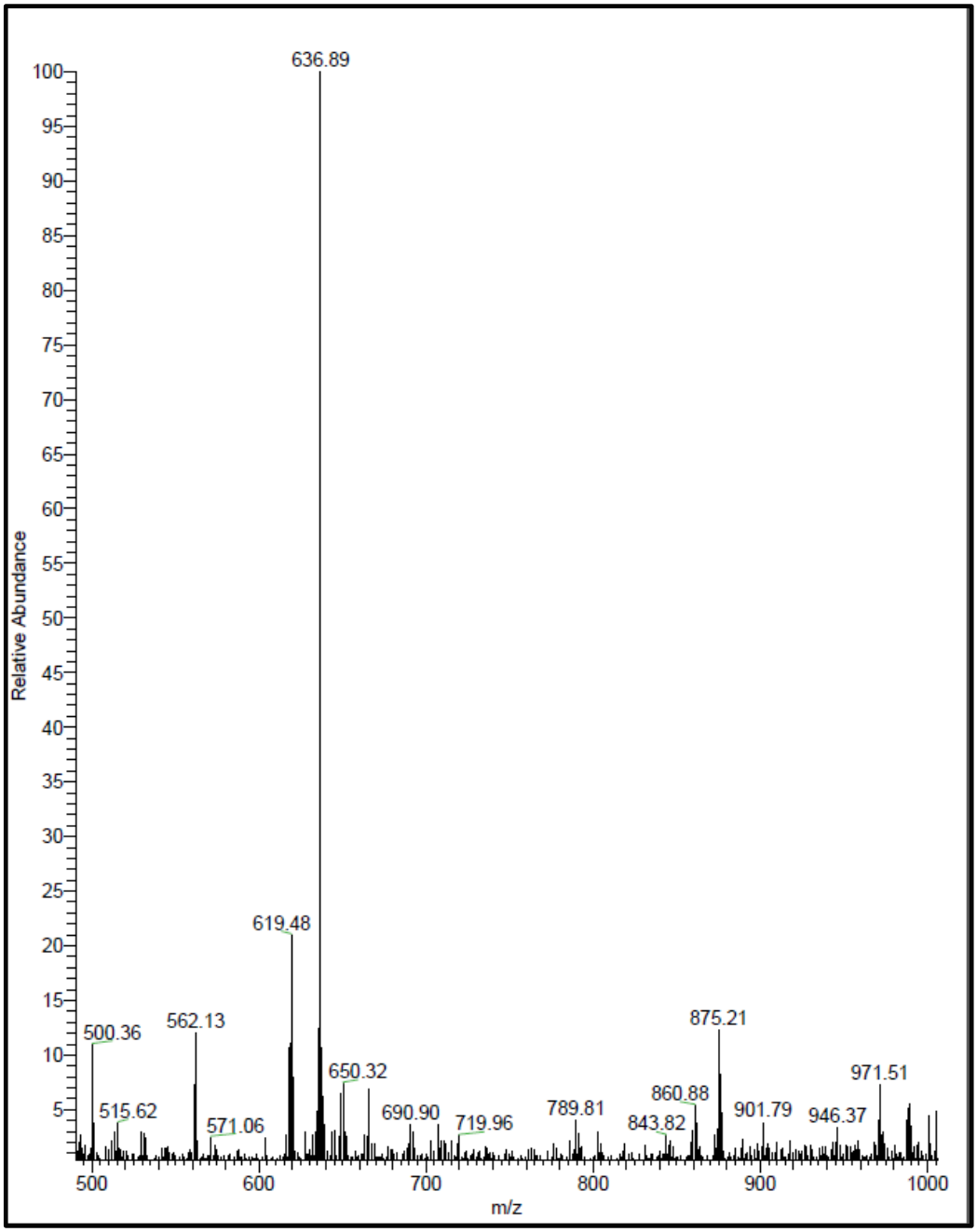

Figure S10. ESI-MS spectrum of $Fe^{III}(BNPA^{Ph_2}O)(OH)(OTf)$ in CH_3CN at 23 °C. ESI-MS(+): *m/z* for $[Fe^{III}(BNPA^{Ph_2}O)(OH)]^+$ 636.85 (*expt.*), 637.05 (*calcd.*). Spray voltage = 0.7 kV.

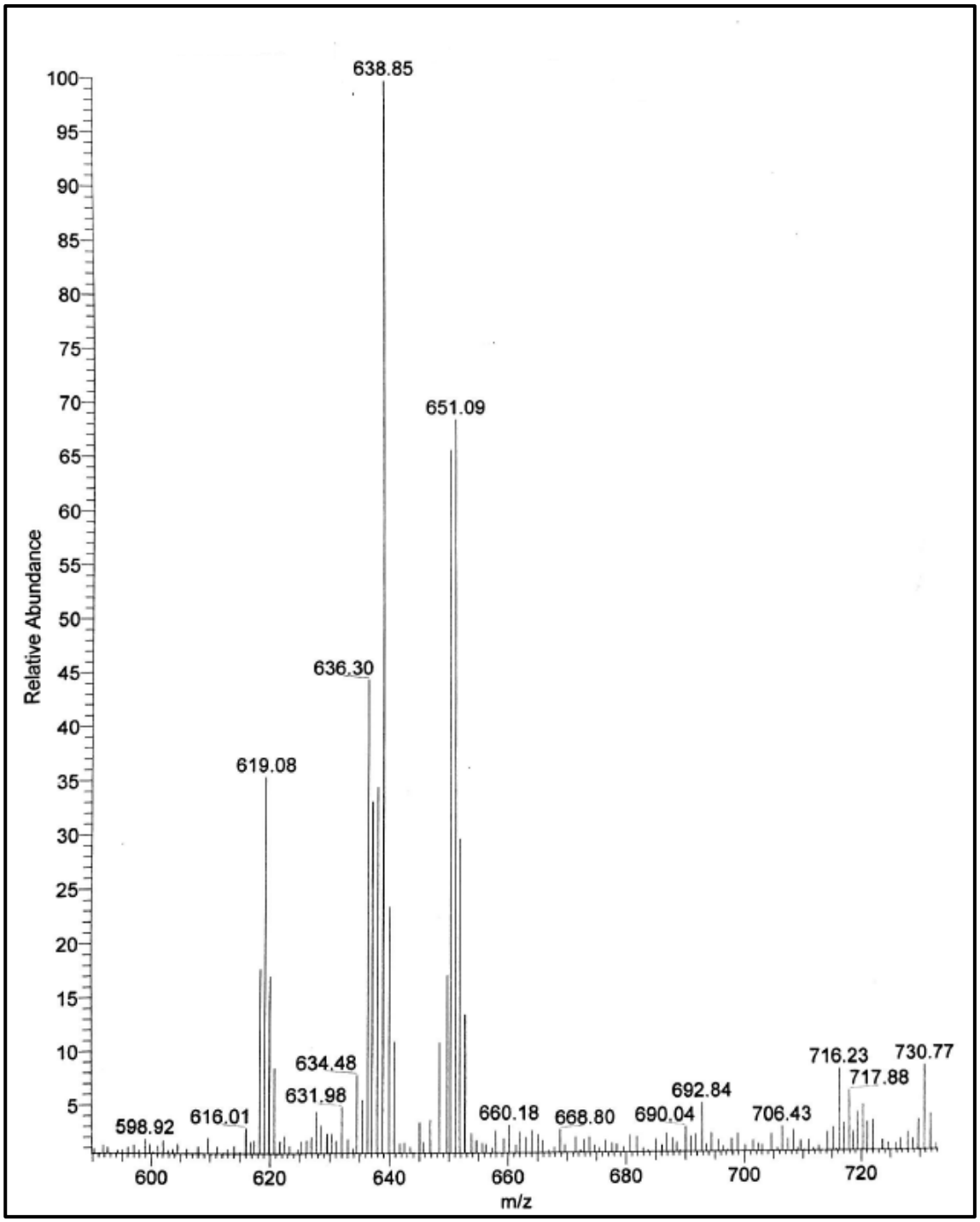

Figure S11. ESI-MS spectrum of $Fe^{III}(BNPA^{Ph_2}O)(^{18}OH)(OTf)$ in CH_3CN at 23 °C. ESI-MS(+): *m/z* for $[Fe^{III}(BNPA^{Ph_2}O)(^{18}OH)]^+$ 638.85 (*expt*), 639.05 (*calcd*), *m/z* = 619.08 corresponds to $[Fe^{II}(BNPA^{Ph_2}O)]^+$ and *m/z* = 651.09 corresponds to $[Fe^{III}(BNPA^{Ph_2}O)(OMe)]^+$, generated from residual MeOH in the ESI-MS instrument. Spray voltage = 0.7 kV.

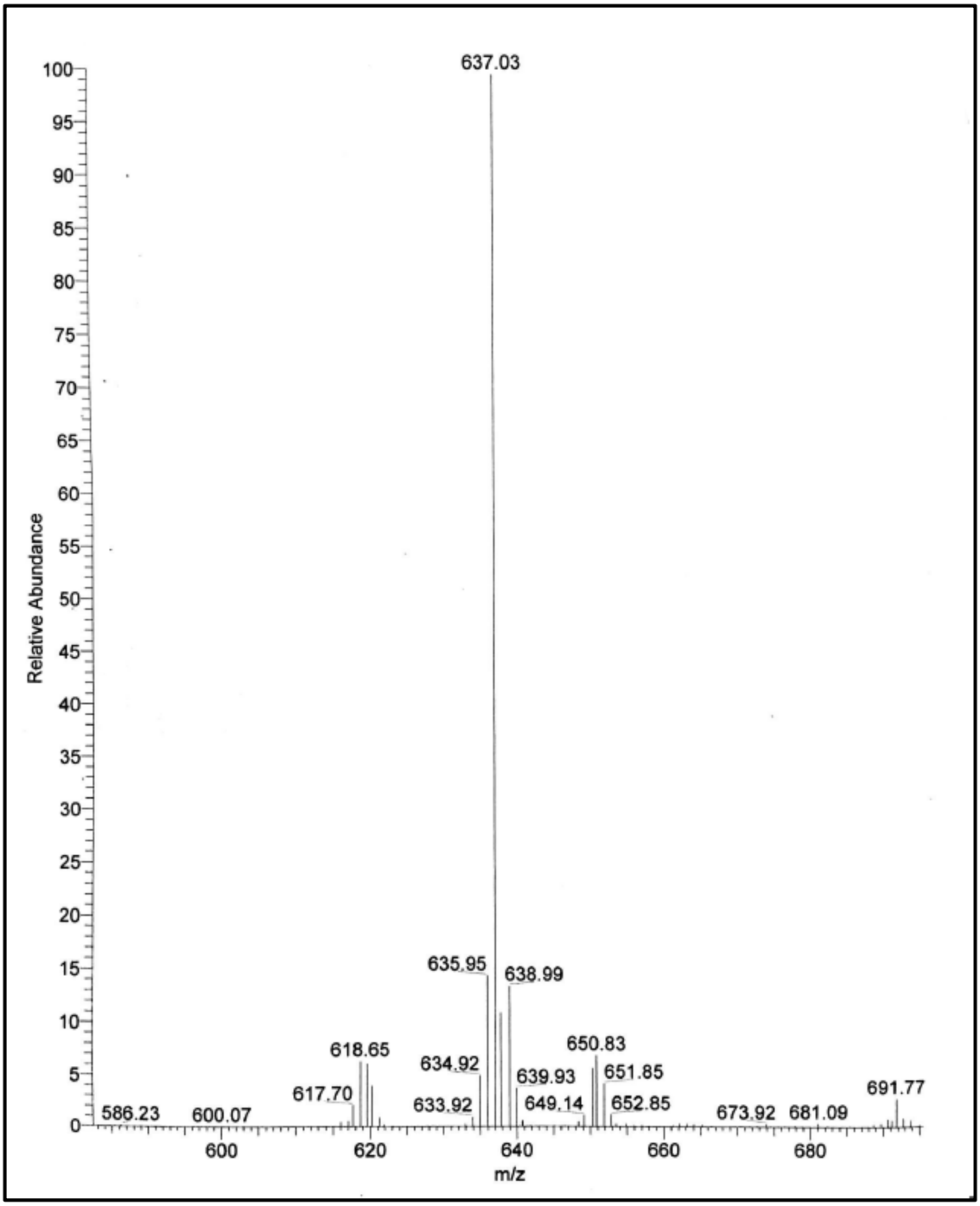

Figure S12. ESI-MS spectrum of the reaction of $Fe^{II}(BNPA^{Ph_2}O)(OTf)$ and O_2 in the presence of $H_2{}^{18}O$ (50 μL) in CH_3CN at 23 °C. ESI-MS(+): *m/z* for $[Fe^{III}(BNPA^{Ph_2}O)(OH)]^+$ 637.03 (*expt*), 637.05 (*calcd*). Spray voltage = 0.7 kV.

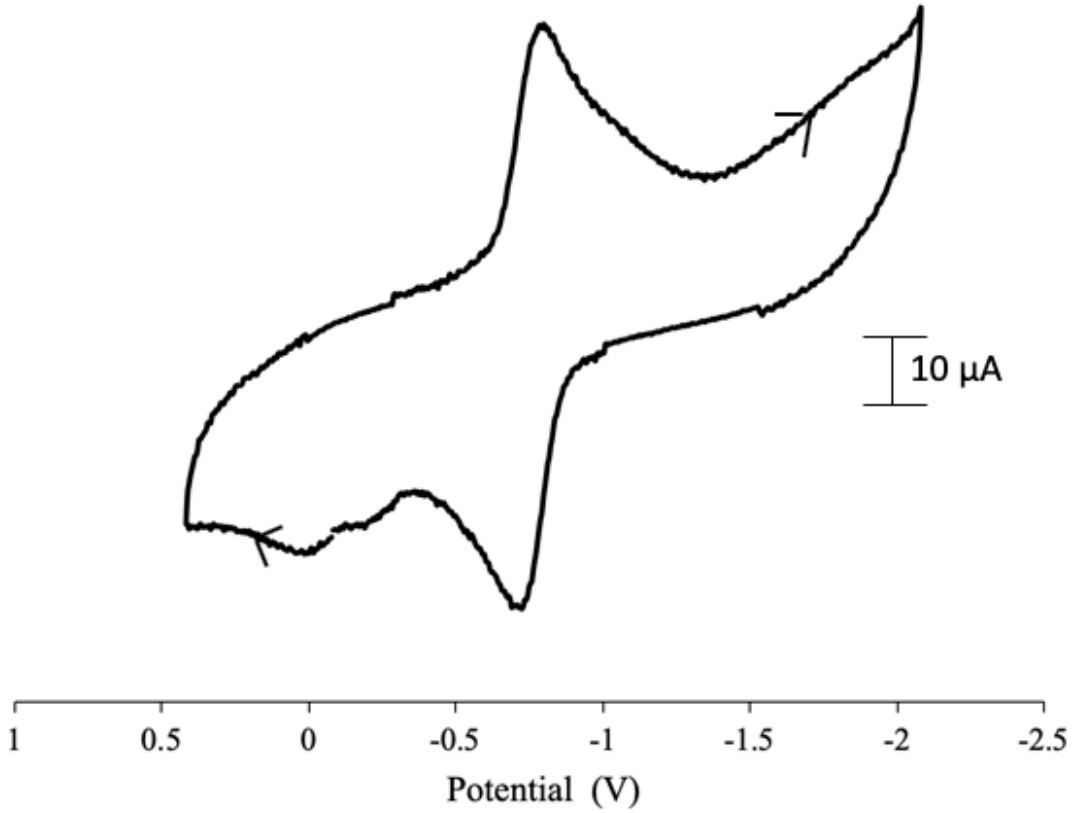

Figure S13. Cyclic voltammogram of **1** (2 mM) in CH_3CN at 23 °C using $^nBu_4NOTf$ (0.1 M) as supporting electrolyte. E_{red} = -0.812 V, E_{ox} = -0.729 V, $E_{1/2}$ = -0.771 V, ΔE_{pp} = 0.083V, scan rate 0.1 V/s. Working electrode: Pt; reference electrode: $Ag/AgNO_3$; counter electrode: Pt wire.

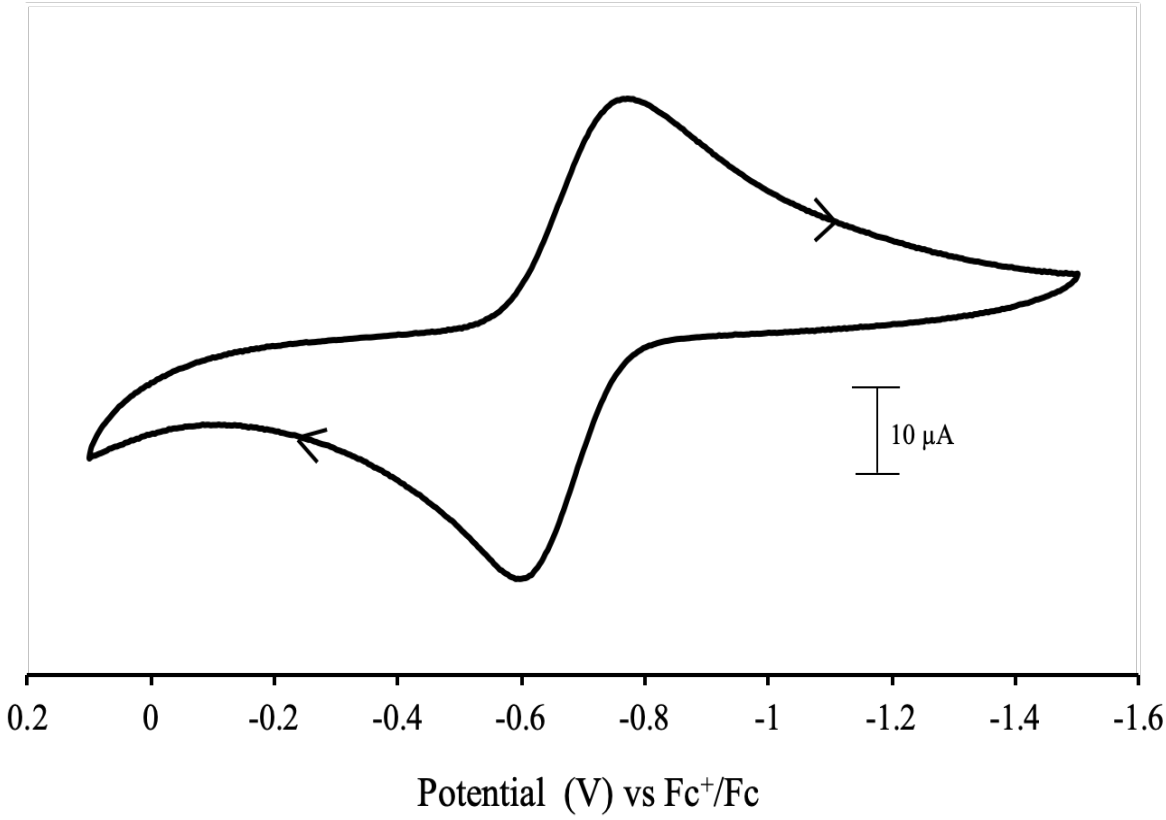

Figure S14. Cyclic voltammogram of **2** (2 mM) in CH_3CN at 23 °C using $^nBu_4NOTf$ (0.1 M) as supporting electrolyte. E_{red} = -0.771 V, E_{ox} = -0.603 V, $E_{1/2}$ = -0.687 V, ΔE_{pp} = 0.17 V, scan rate 0.1 V/s. Working electrode: glassy carbon; reference electrode: $Ag/AgNO_3$; counter electrode: Pt wire.

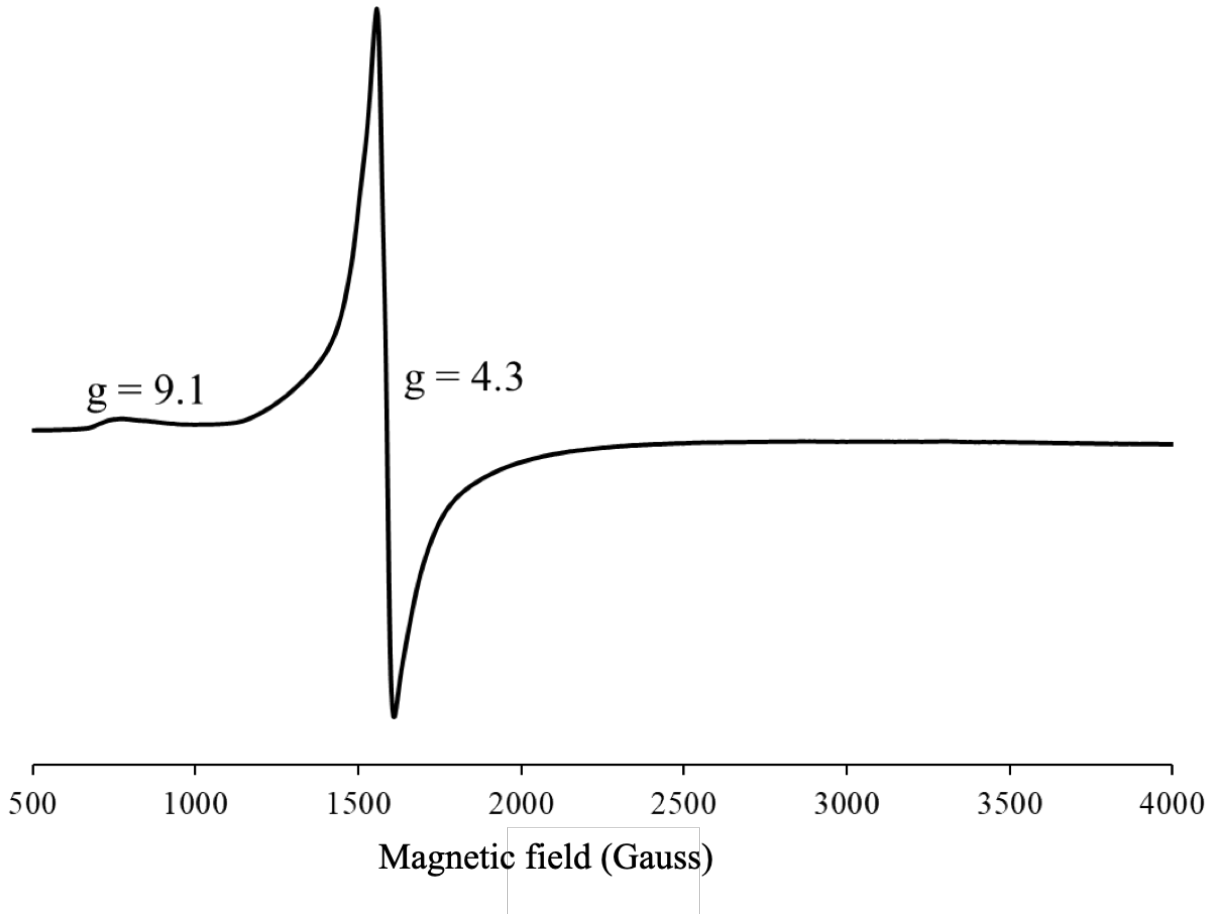

Figure S15. X-band EPR spectrum of **2** (4 mM) at 20 K in CH_3CN. Frequency 9.2617 GHz, modulation amplitude 10 G, modulation frequency 100 kHz, attenuation 20 dB, receiver gain 5.02 x 10^3.

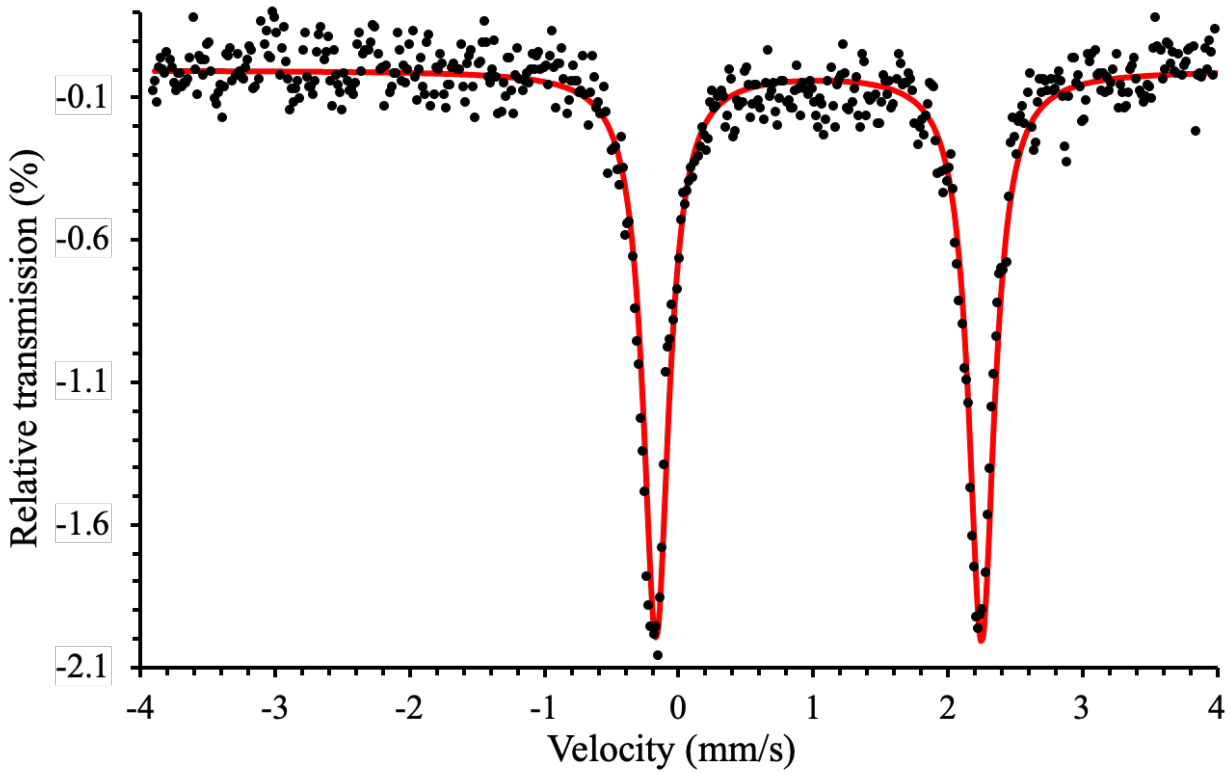

Figure S16. Zero-field ^{57}Fe Mössbauer spectrum of solid **1** (natural abundance) dispersed in BN matrix at 80 K. Experimental data = black circles and best fit = red line, with parameters δ = 1.03 mm s^{-1}, $|\Delta E_Q|$ = 2.42 mm s^{-1}, $\Gamma_R = \Gamma_L$ = 0.3, χ^2 = 0.738.

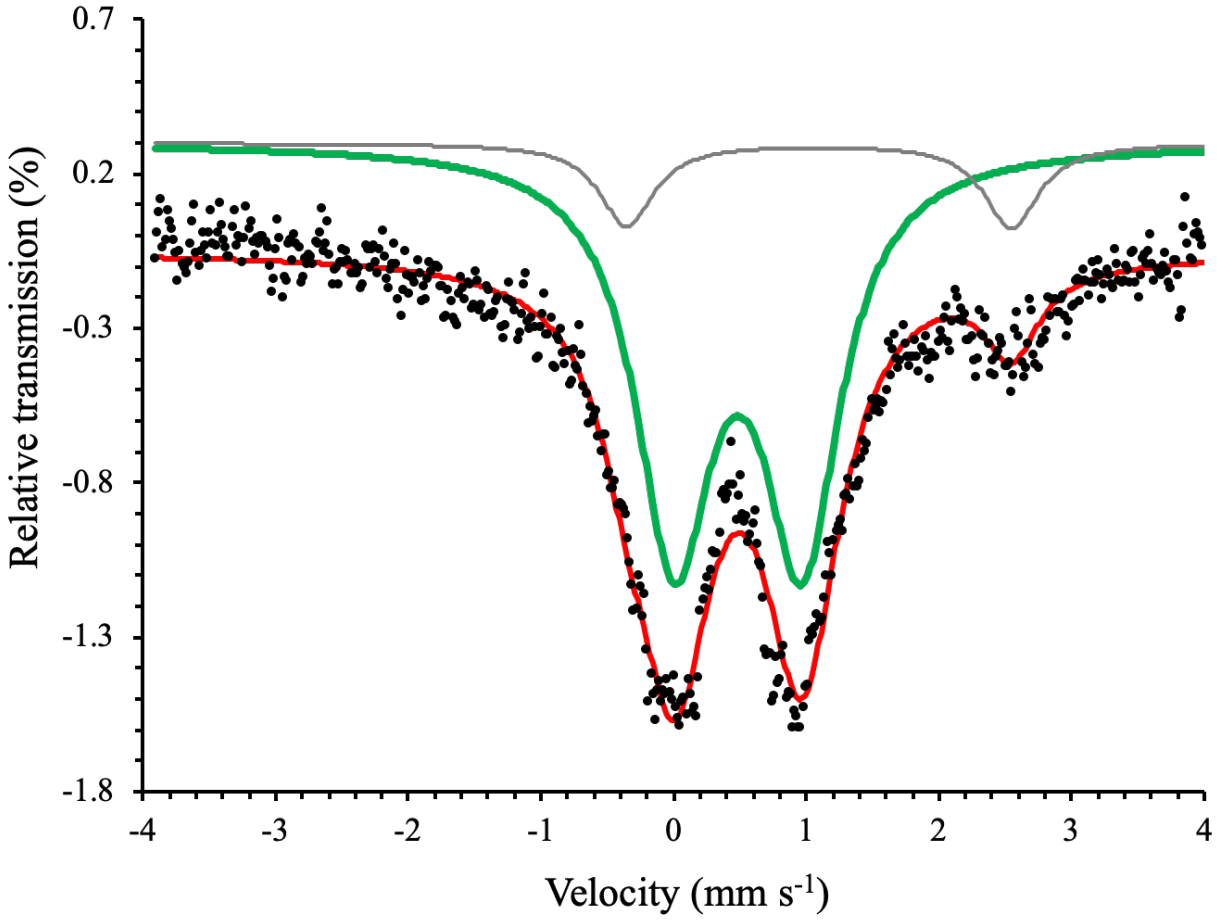

Figure S17. Zero-field ^{57}Fe Mössbauer spectrum of solid **2** (natural abundance) dispersed in BN matrix at 80 K. Experimental data = black circles and best fit = red line. Subsite 1 = green line, with parameters δ = 0.47 mm s^{-1}, $|\Delta E_Q|$ = 0.97 mm s^{-1}, $\Gamma_R = \Gamma_L$ = 0.7, % I = 90 (major species, **2**) and subsite 2 = gray line, with parameters δ = 1.05 mm s^{-1}, $|\Delta E_Q|$ = 2.91 mm s^{-1}, $\Gamma_R = \Gamma_L$ = 0.6, % I = 10 (high-spin Fe^{II} impurity).

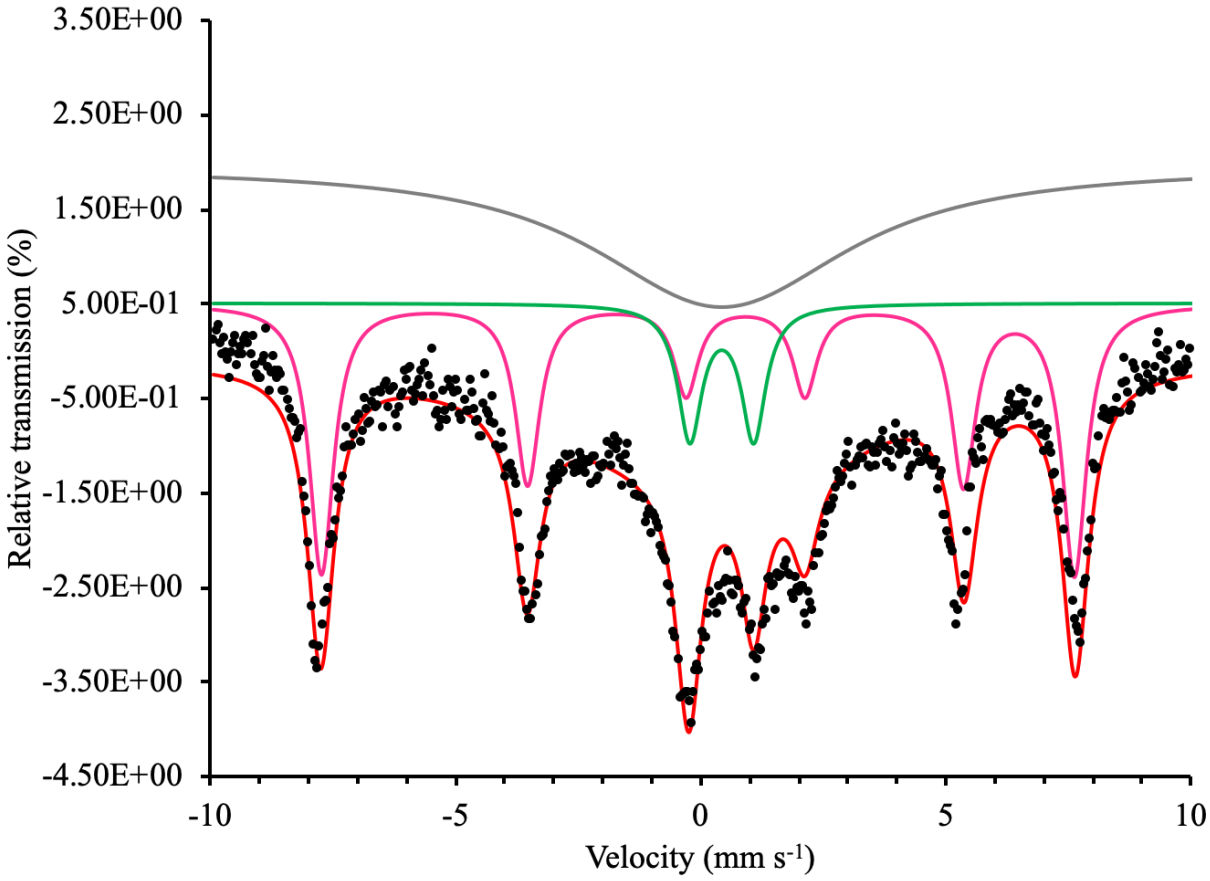

Figure S18. Zero-field ^{57}Fe Mössbauer spectra of solid **2** frozen in CH_3CN at 5 K. Experimental data = black circels, best fit = red line, slow relaxing species = pink line with parameters δ = 0.44 and ΔE_Q= -0.97 mm s^{-1}, Rel. Area = 0.40 and fast relaxing species = green line with parameters δ = 0.44 and $|\Delta E_Q|$ = 1.30 mm s^{-1}, Rel. Area = 0.10. A third, broad subcomponent with δ = 0.44 mm s^{-1}, $|\Delta E_Q|$ = 1.00 mm s^{-1}, $\Gamma_R = \Gamma_L$ = 6.0, (grey line) was added to represent the intermediate relaxation of the doublet, accounting for the observation that complex **2** is not fully in a slow relaxation regime at 5 K. To fit the slow relaxing species, an internal magnetic field (H_{int}) 478 kG was included in the fit.

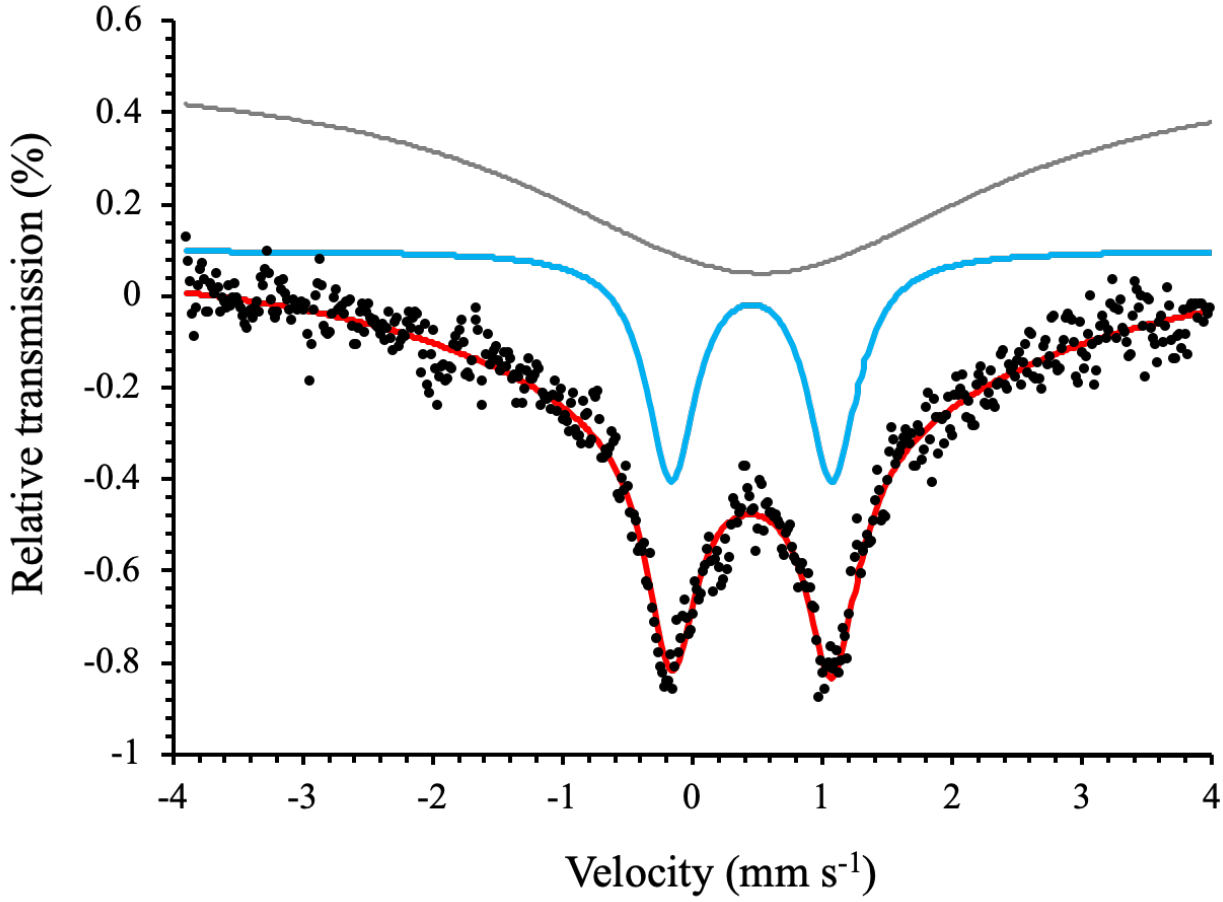

Figure S19. Zero-field ^{57}Fe Mössbauer spectrum of ^{57}Fe-labelled **2** frozen in 2-MeTHF at 80 K. Experimental data = black circles, best fit = red line, which is composed of one subcomponent with parameters $\delta = 0.47$ mm s^{-1}, $|\Delta E_Q| = 1.24$ mm s^{-1}, $\Gamma_R = \Gamma_L = 0.6$, (blue line), and a second, broad subcomponent with $\delta = 0.40$ mm s^{-1}, $|\Delta E_Q| = 1.00$ mm s^{-1}, $\Gamma_R = \Gamma_L = 4.0$, (grey line). The latter component was added to represent the intermediate relaxation of the doublet at 80 K. The conclusion that the broadness in the data at 80 K comes from intermediate relaxation is supported by the observed six-line pattern in the Mössbauer spectrum for **2** at 5 K (Figure S18).

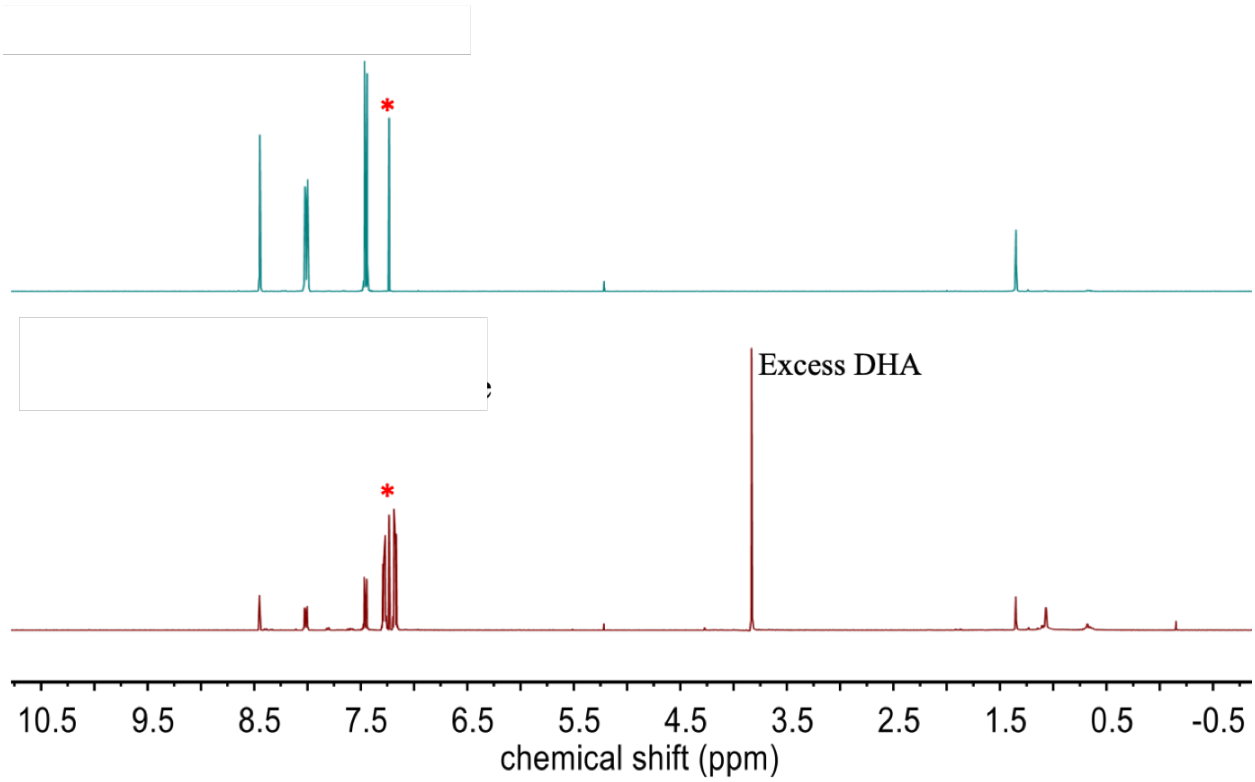

Figure S20. ^{1}H NMR spectra of anthracene (top) and reaction mixture of complex **1** and excess O_2 with 9,10-dihydroanthracene (10 equiv) in $CDCl_3$ (bottom). Residual solvent $CHCl_3$ peak is marked with an asterisk (*).

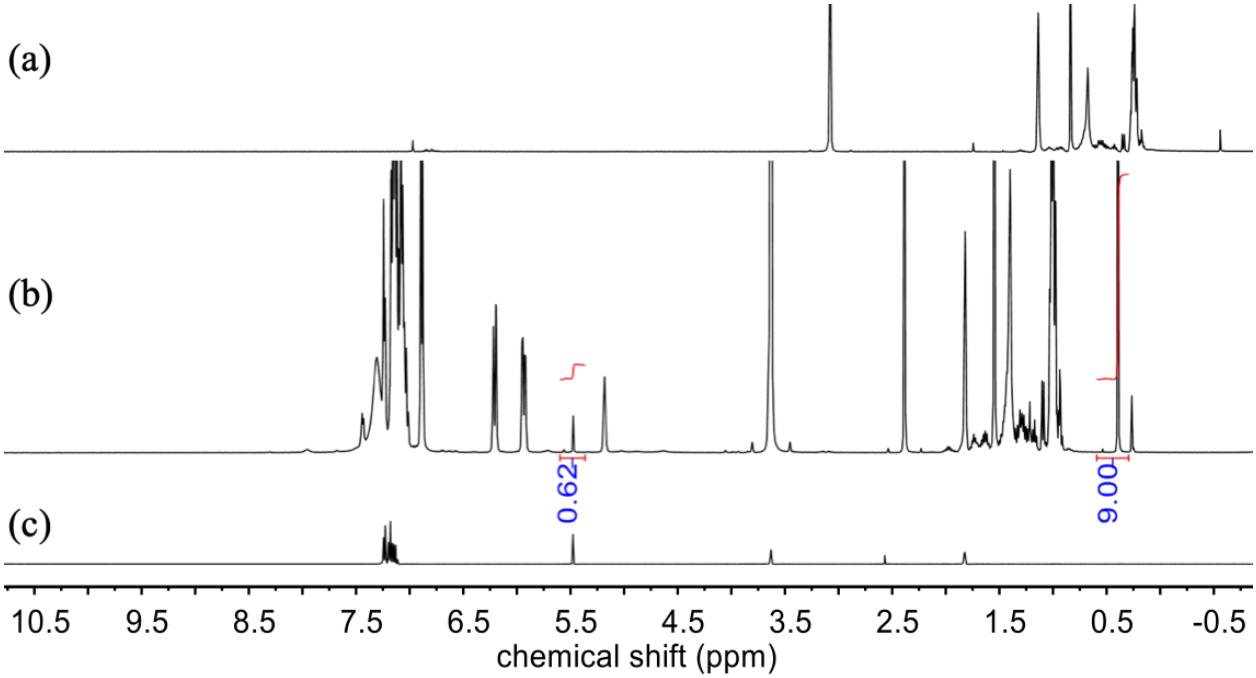

Figure S21. Quantification by ^{1}H NMR spectroscopy of Ph_3COH in the reaction with **2** and $Ph_3C\bullet$ in THF-d_8 at 23 °C using the internal standard trimethylphenylsilane, where spectra are shown for (a) pure **2,** (b) reaction mixture of **2** + $Ph_3C\bullet$ and (c) pure Ph_3COH. The peak at δ 5.50 ppm corresponds to the -OH peak of Ph_3COH and the peak at δ 0.28 ppm corresponds to the internal standard.

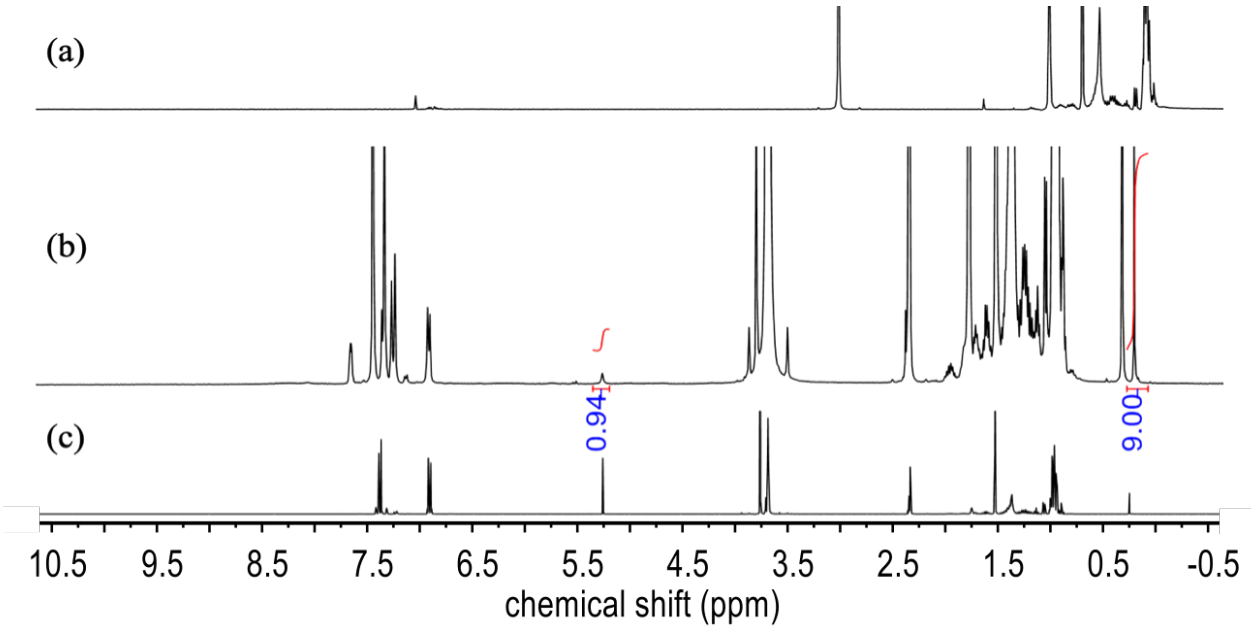

Figure S22. Quantification by ^{1}H NMR spectroscopy of (p-OMe-C_6H_4)$_3$COH in the reaction with **2** and (p-OMe-C_6H_4)$_3$C• in THF-d_8/toluene-d_8 (5/2 v/v) at 23 °C using the internal standard trimethylphenylsilane, where spectra are shown in THF-d_8/toluene-d_8 (5/2 v/v) for (a) pure **2,** (b) reaction mixture of **2** + (p-OMe-C_6H_4)$_3$C• and (c) pure (p-OMe-C_6H_4)$_3$COH. The peak at δ 5.24 ppm corresponds to the -OH peak of (p-OMe-C_6H_4)$_3$COH and the peak at δ 0.25 ppm corresponds to the internal standard.

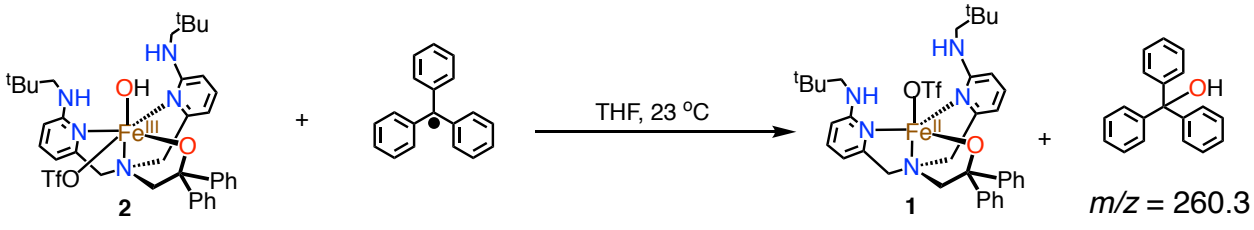

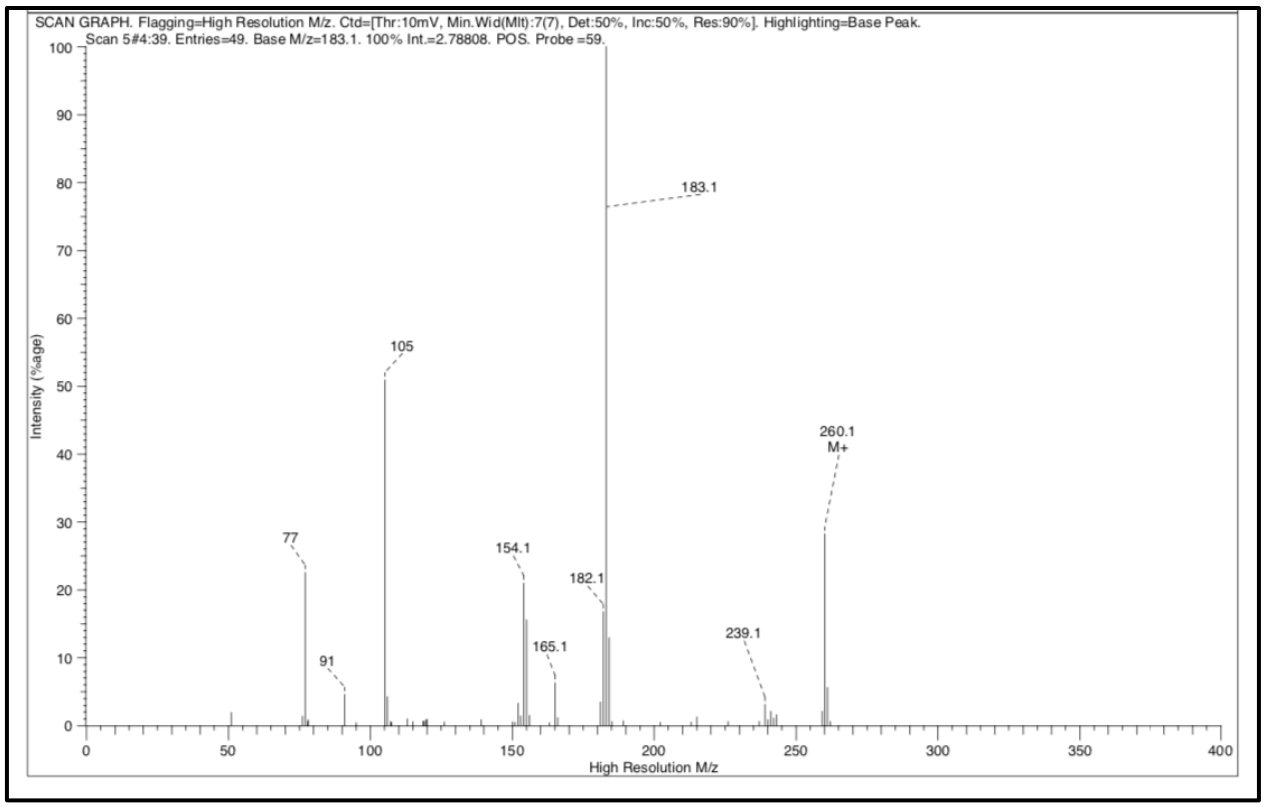

Figure S23. EI-MS spectrum of the reaction mixture of **2** and $Ph_3C\bullet$ in THF at 23 °C. EI-MS: *m/z* for the product $(p\text{-OMe-}C_6H_4)_3COH$ 260.1 (*expt*), 260.2 (*calcd*).

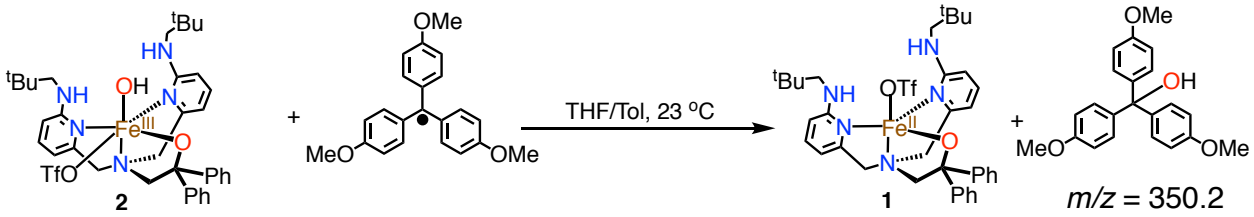

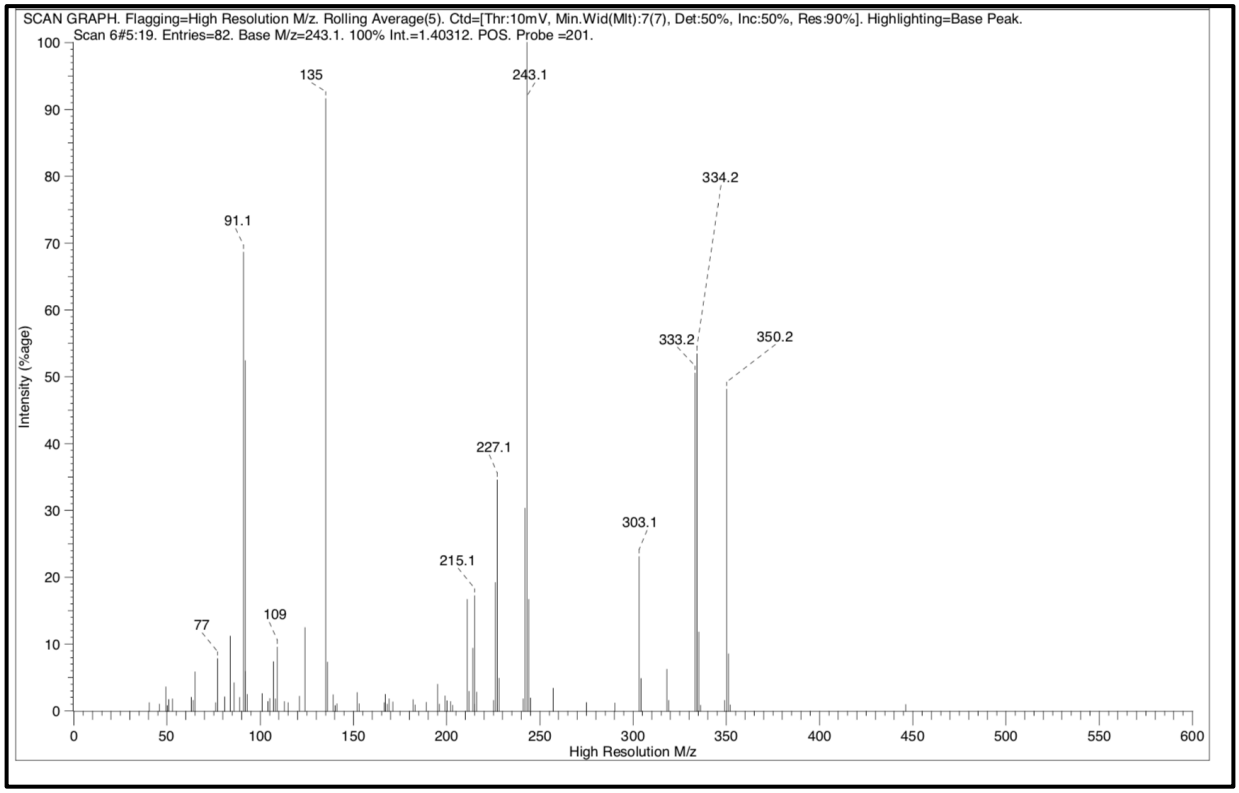

Figure S24. EI-MS spectrum of the reaction mixture of **2** and $(p\text{-OMe-C}_6\text{H}_4)_3\text{C}\bullet$ in THF/toluene (5/2 v/v) at 23 °C. EI-MS: *m/z* for the product $(p\text{-OMe-C}_6\text{H}_4)_3\text{COH}$ 350.2 (*expt*), 350.15 (*calcd*).

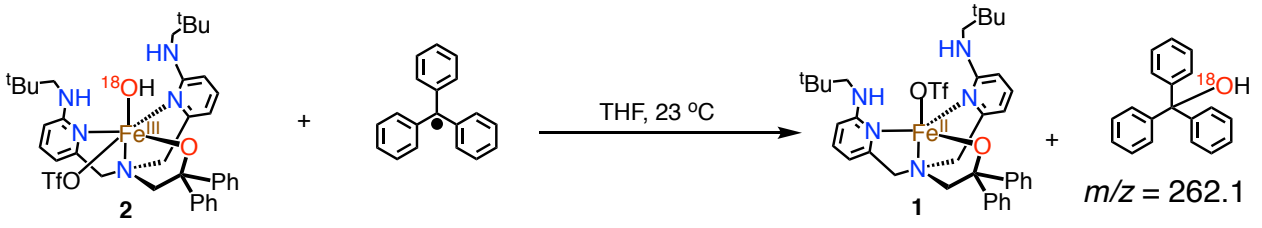

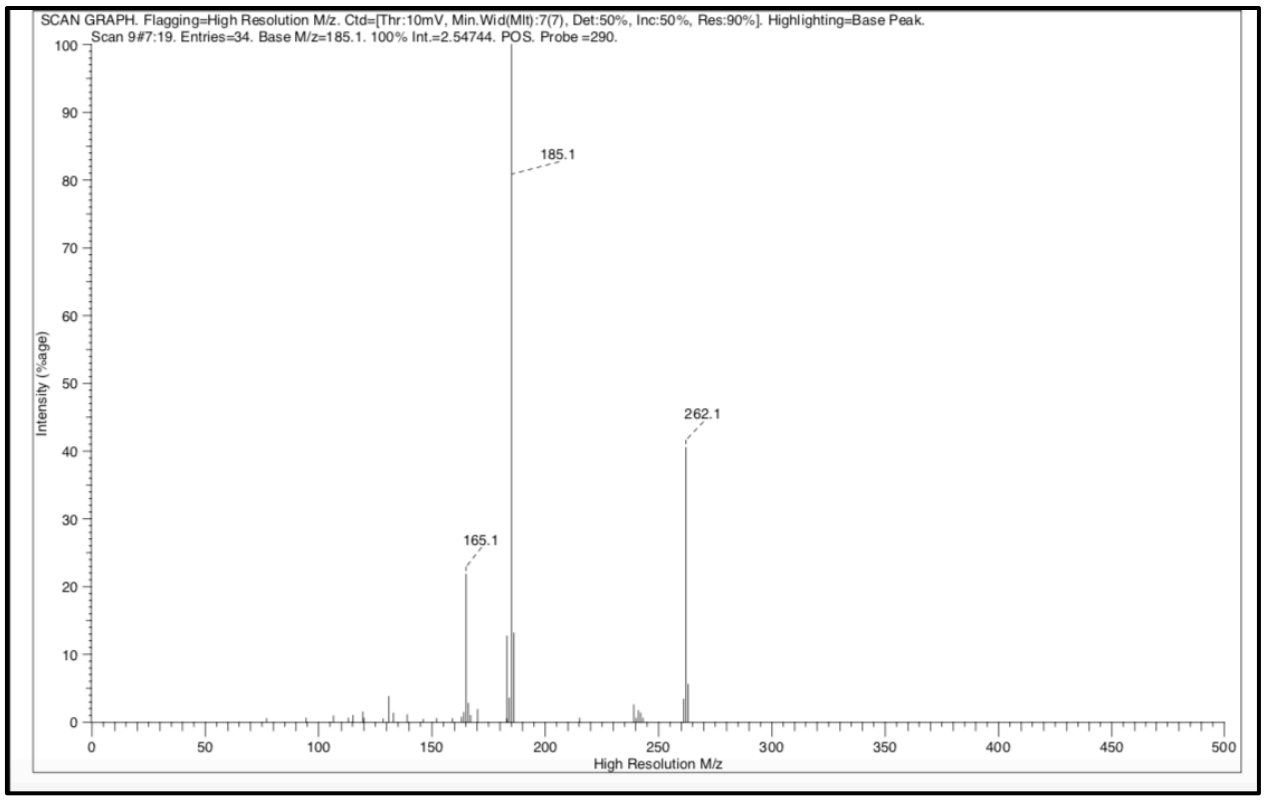

Figure S25. EI-MS spectrum of the reaction mixture of ^{18}O labelled **2** and $Ph_3C\bullet$ in THF at 23 °C. EI-MS: *m/z* for the product $Ph_3C^{18}OH$ 262.1 (*expt*), 262.2 (*calcd*). The ^{18}O labelled **2** was prepared by adding 80 µL of $H_2{}^{18}O$ into a CH_3CN solution of **2** followed by stirring for 3 h. Solvent was removed under vacuum and excess water was removed by drying under vacuum over P_2O_5 for 12 h prior to the radical reaction.

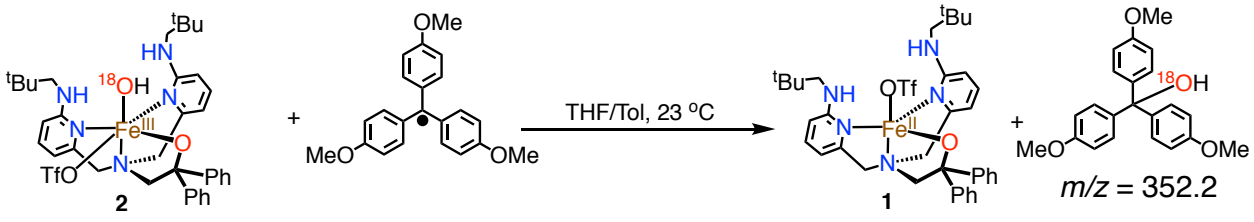

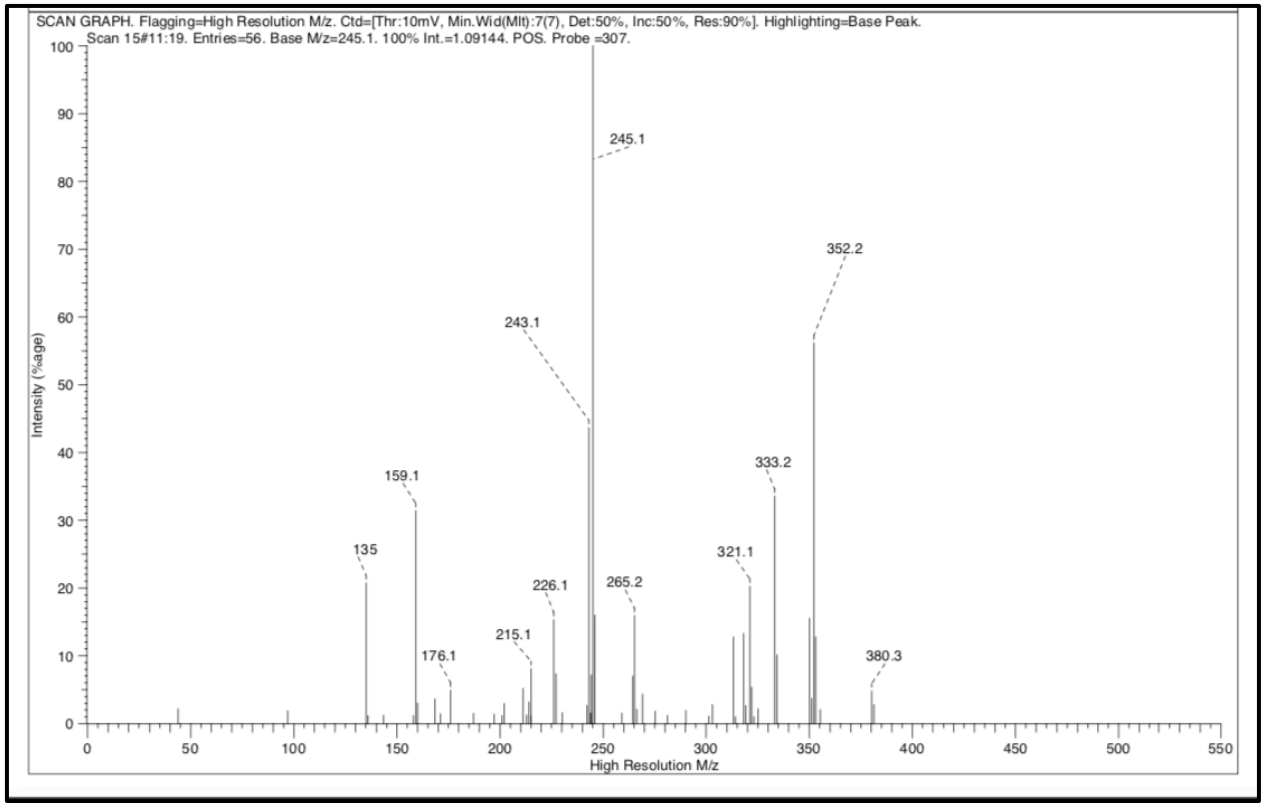

Figure S26. EI-MS spectrum of the reaction mixture of ^{18}O labelled **2** and $(p\text{-OMe-C}_6H_4)_3C\bullet$ in THF/toluene (5/2 v/v) at 23 °C. EI-MS: *m/z* for the product $(p\text{-OMe-C}_6H_4)_3C^{18}OH$ 352.2 (*expt*), 352.2 (*calcd*). The ^{18}O labelled **2** was prepared by adding 80 μL of $H_2{}^{18}O$ into a CH_3CN solution of **2** followed by stirring for 3 h. Solvent was removed under vacuum and excess water was removed by drying under vacuum over P_2O_5 for 12 h prior to the radical reaction.

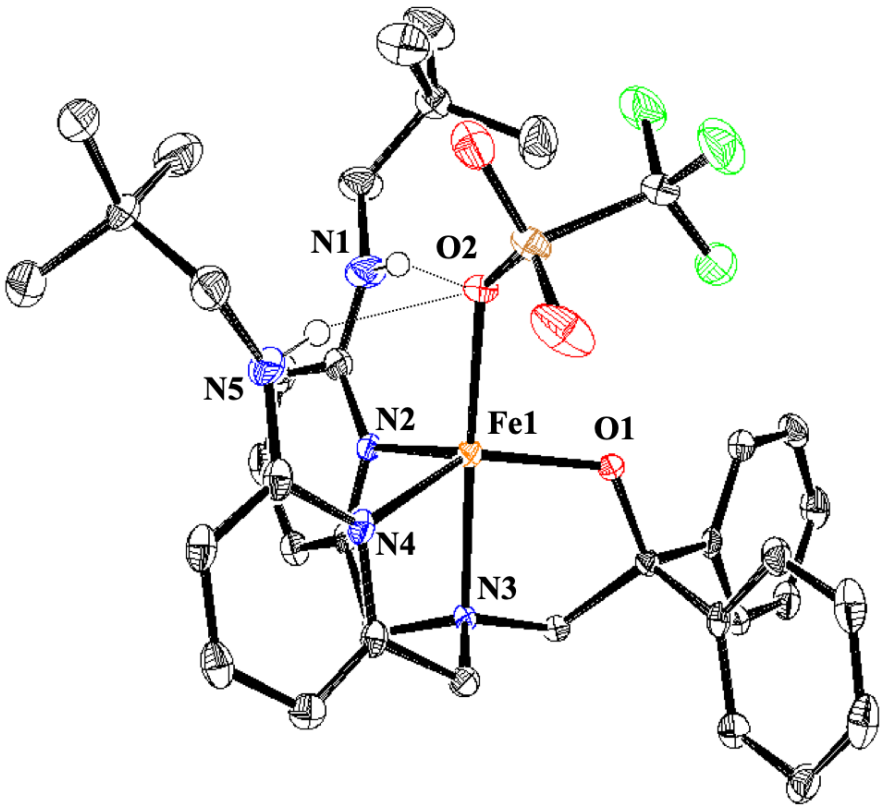

Figure S27. Displacement ellipsoid plot (50% probability) of $Fe^{II}(BNPA^{Ph_2}O)(OTf)$ at 110(2) K. H-atoms except those attached to N1 and N5 are removed for clarity. Selected bond lengths (Å) and bond angles (°) Fe1–N2 2.1527(16), Fe1–N3 2.1731(16), Fe1–N4 2.1745(16), Fe1–O1 1.9003(13), Fe1–O2 2.1598(16), N1–O2 3.026(2), N5–O2 3.116(2) , N3–Fe1–N4 77.45(6), N2–Fe1–N4 99.37(6), N2–Fe1–N3 78.79(6), N2–Fe1–O1 114.71(6), N3–Fe1–O1 82.67(6), N4–Fe1–O1 136.05(6), N4–Fe1–O2 101.58(7), N2–Fe1–O2 105.14(7), O1–Fe1–O2 95.61(6), N3–Fe1–O2 176.07(6), N1–H1–O2 166(2), N5–H5–O2 161(2).

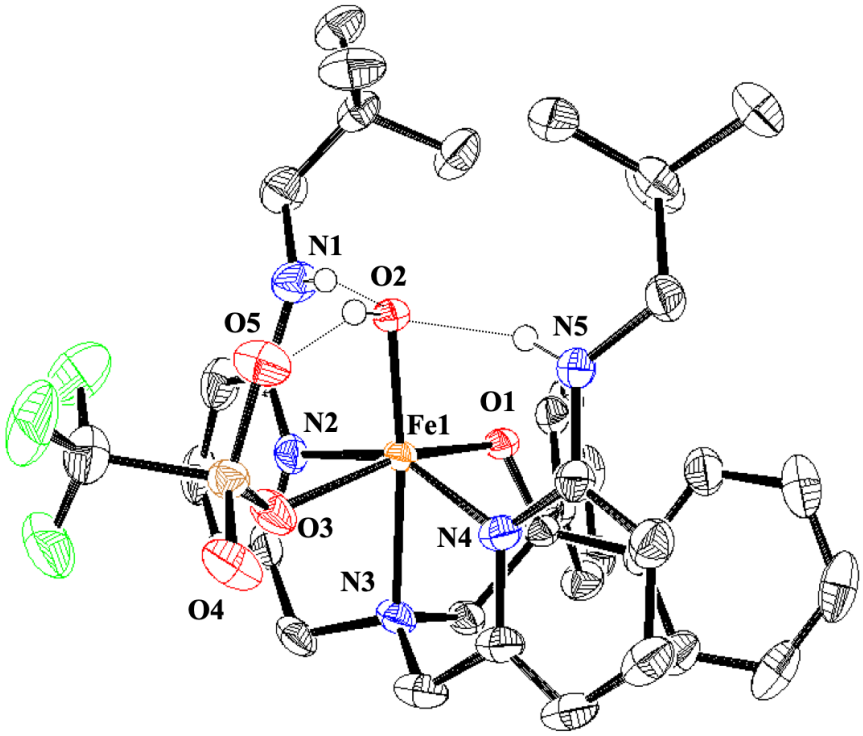

Figure S28. Displacement ellipsoid plot (50% probability) of $Fe^{III}(BNPA^{Ph_2}O)(OH)(OTf)$ at 110(2) K. H-atoms except those attached to N1, N5 and O2 are removed for clarity . Selected bond lengths (Å) and bond angles (°) Fe1–N2 2.1605(19), Fe1–N3 2.1660(16), Fe1–N4 2.1593(18), Fe1–O1 1.8558(13), Fe1–O2 1.8797(13), Fe1–O3 2.2017(14), N1–O2 2.831(3), N5–O2 2.857(2), N2–Fe1–N3 77.74(7), N3–Fe1–N4 78.04(6), N2–Fe1–N4 154.51(6), N4–Fe1–O1 92.86(6), N3–Fe1–O1 85.00(6), N2–Fe1–O1 92.85(6), N4–Fe1–O3 83.88(7), N3–Fe1–O3 81.53(6), O1–Fe1–O2 101.82(6), N3–Fe1–O3 81.53(6), , O2–Fe1–N3 173.18(6), O2–Fe1–N4 101.62(6), , O3–Fe1–O2 91.66(6), N1–H1–O2 166(3), N5–H5–O2 162(2), O5–H2–O2 160(3).

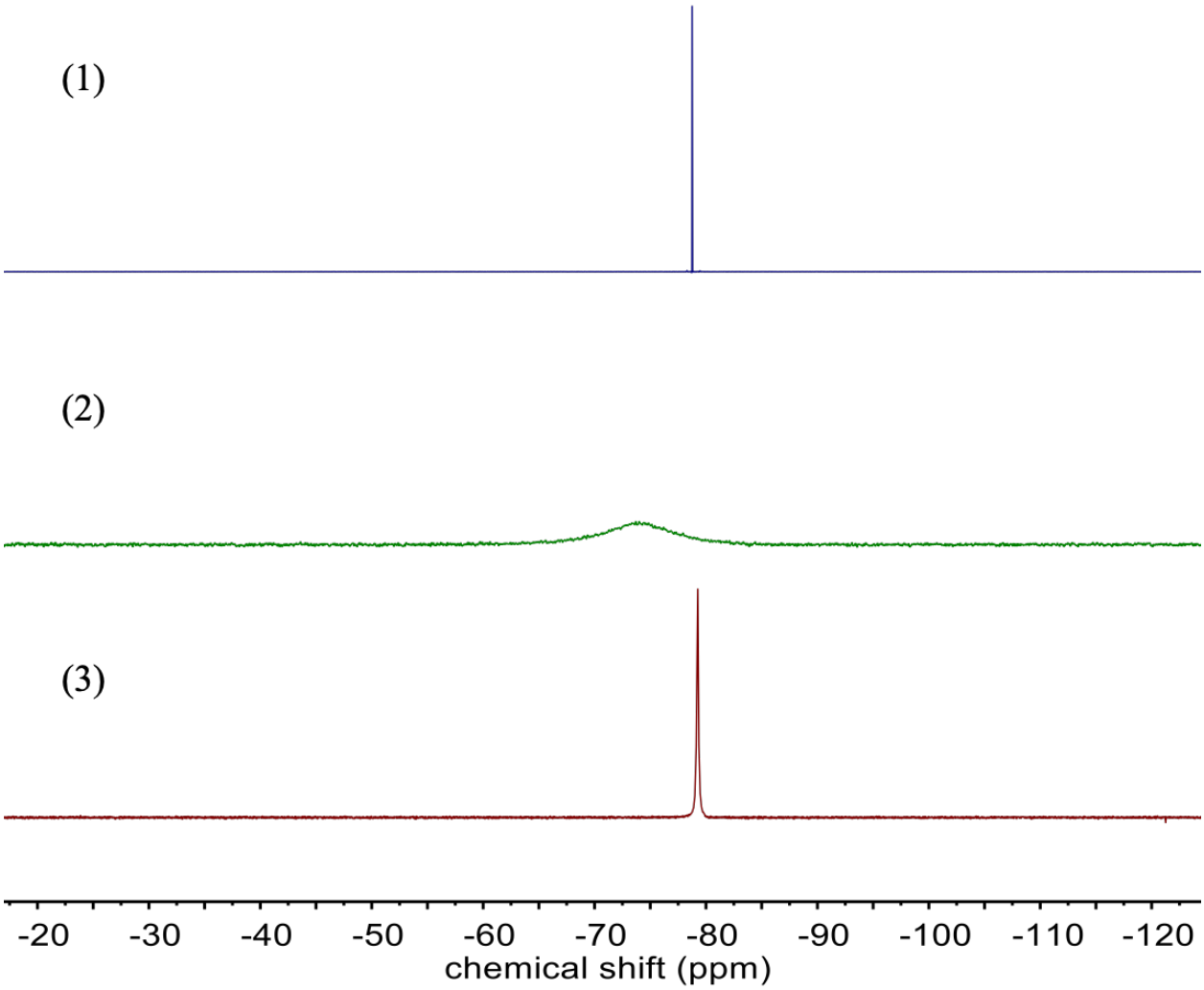

Figure S29. ^{19}F NMR spectra of (1) $^{n}Bu_4NOTf$ in CD_3CN, (2) complex **1** in THF-d_8 and (3) complex **1** in CD_3CN.

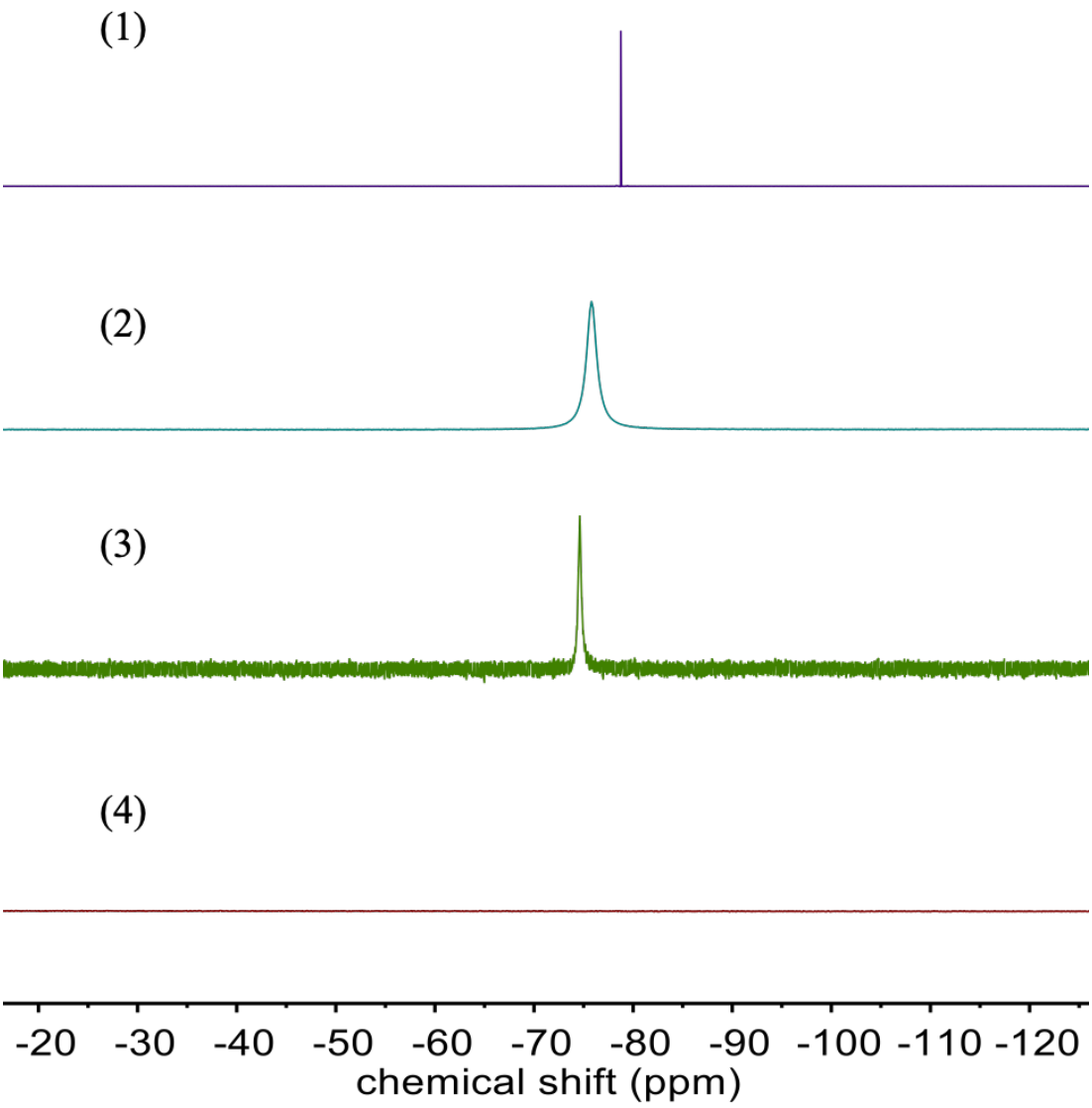

Figure S30. ^{19}F NMR spectra of (1) $^{n}Bu_4NOTf$ in CD_3CN, (2) complex **2** in THF-d_8 in the presence of excess $^{n}Bu_4NOTf$, (3) complex **2** in CD_3CN and (4) complex **2** in THF-d_8.

G. References

1. Hagen, K. S., Iron(II) Triflate Salts as Convenient Substitutes for Perchlorate Salts: Crystal Structures of $[Fe(H_2O)_6](CF_3SO_3)_2$ and $Fe(MeCN)_4(CF_3SO_3)_2$. *Inorg. Chem.* **2000,** *39*, 5867-5869.
2. Pike, S. J.; De Poli, M.; Zawodny, W.; Raftery, J.; Webb, S. J.; Clayden, J., Diastereotopic fluorine substituents as ^{19}F NMR probes of screw-sense preference in helical foldamers. *Org. Biomol. Chem.* **2013,** *11*, 3168-3176.
3. Zaragoza, J. P. T.; Yosca, T. H.; Siegler, M. A.; Moënne-Loccoz, P.; Green, M. T.; Goldberg, D. P., Direct Observation of Oxygen Rebound with an Iron-Hydroxide Complex. *J. Am. Chem. Soc.* **2017,** *139*, 13640-13643.
4. Jang, E. S.; McMullin, C. L.; Käß, M.; Meyer, K.; Cundari, T. R.; Warren, T. H., Copper(II) Anilides in sp^3 C-H Amination. *J. Am. Chem. Soc.* **2014,** *136*, 10930-10940.
5. Fulmer, G. R.; Miller, A. J. M.; Sherden, N. H.; Gottlieb, H. E.; Nudelman, A.; Stoltz, B. M.; Bercaw, J. E.; Goldberg, K. I., NMR Chemical Shifts of Trace Impurities: Common Laboratory Solvents, Organics, and Gases in Deuterated Solvents Relevant to the Organometallic Chemist. *Organometallics* **2010,** *29*, 2176-2179.
6. Sahu, S.; Widger, L. R.; Quesne, M. G.; de Visser, S. P.; Matsumura, H.; Moënne-Loccoz, P.; Siegler, M. A.; Goldberg, D. P., Secondary Coordination Sphere Influence on the Reactivity of Nonheme Iron(II) Complexes: An Experimental and DFT Approach. *J. Am. Chem. Soc.* **2013,** *135*, 10590-10593.
7. Neese, F., The ORCA program system. *Wiley Interdiscip. Rev.: Comput. Mol. Sci.* **2012,** *2*, 73-78.
8. Perdew, J. P., Density-functional approximation for the correlation energy of the inhomogeneous electron gas. *Phys. Rev. B* **1986,** *33*, 8822-8824.
9. McLean, A. D.; Chandler, G. S., Contracted Gaussian basis sets for molecular calculations. I. Second row atoms, Z=11–18. *J. Chem. Phys.* **1980,** *72*, 5639-5648.
10. Hehre, W. J.; Lathan, W. A., Self-Consistent Molecular Orbital Methods. XIV. An Extended Gaussian-Type Basis for Molecular Orbital Studies of Organic Molecules. Inclusion of Second Row Elements. *J. Chem. Phys.* **1972,** *56*, 5255-5257.
11. Stephens, P. J.; Devlin, F. J.; Chabalowski, C. F.; Frisch, M. J., Ab Initio Calculation of Vibrational Absorption and Circular Dichroism Spectra Using Density Functional Force Fields. *J. Phys. Chem.* **1994,** *98*, 11623-11627.
12. Römelt, M.; Ye, S.; Neese, F., Calibration of Modern Density Functional Theory Methods for the Prediction of ^{57}Fe Mössbauer Isomer Shifts: Meta-GGA and Double-Hybrid Functionals. *Inorg. Chem.* **2009,** *48*, 784-785.
13. Weigend, F.; Ahlrichs, R., Balanced basis sets of split valence, triple zeta valence and quadruple zeta valence quality for H to Rn: Design and assessment of accuracy. *Phys. Chem. Chem. Phys.* **2005,** *7*, 3297-3305.
14. Pápai, M.; Vankó, G., On Predicting Mössbauer Parameters of Iron-Containing Molecules with Density-Functional Theory. *J. Chem. Theory Comput.* **2013,** *9*, 5004-5020.
15. Ogo, S.; Yamahara, R.; Roach, M.; Suenobu, T.; Aki, M.; Ogura, T.; Kitagawa, T.; Masuda, H.; Fukuzumi, S.; Watanabe, Y., Structural and Spectroscopic Features of a cis (Hydroxo)-FeIII-(Carboxylato) Configuration as an Active Site Model for Lipoxygenases. *Inorg. Chem.* **2002,** *41*, 5513-5520.
16. Soo, H. S.; Komor, A. C.; Iavarone, A. T.; Chang, C. J., A Hydrogen-Bond Facilitated Cycle for Oxygen Reduction by an Acid- and Base-Compatible Iron Platform. *Inorg. Chem.* **2009,** *48*, 10024-10035.
17. Mukherjee, J.; Lucas, R. L.; Zart, M. K.; Powell, D. R.; Day, V. W.; Borovik, A. S., Synthesis, Structure, and Physical Properties for a Series of Monomeric Iron(III) Hydroxo Complexes with Varying Hydrogen-Bond Networks. *Inorg. Chem.* **2008,** *47*, 5780-5786.